TITLE

Proto-oncogene cSrc-mediated RBM10 phosphorylation arbitrates anti-hypertrophy gene program in the heart and controls cardiac hypertrophy

INTRODUCTION

RNA binding proteins (RBP) are group of proteins that regulate various aspects of RNA metabolism and gene expression involved in almost all cellular functions[14, 19, 26]. One such protein RNA binding motif protein 10 (RBM10) is emerging as a crucial regulator in complex human diseases such as cancer or heart failure [7, 29, 46]. RBM10 is highly conserved in mammals and binds RNA sequences but with a preference to G and U-rich sequences [12, 30, 37, 70]. The gene encoding for RBM10 maps to the X chromosome at position p11.23 and is expressed ubiquitously [29, 46]. RBM10 contains at least five distinct types of domains including two RNA recognition motifs (RRM), two zinc finger motifs, an OCRE domain, a KEKE motif domain, and a G-patch domain[30, 59]. The RRM1, ZnF and RRM2 domains together participate in RNA binding, while the NLS at the C-terminal end, RRM1, OCRE domain contributes to nuclear localisation[12, 30, 59, 69, 72]. The OCRE, KEKE and G-patch domains interact with spliceosomal complex contributing to splicing function [25, 49, 70]. While RBM10 is largely localised to nuclear speckles, it is also detected in the cytoplasm in response to cellular signals[69, 72, 73]. In somatic cells, RBM10 is transcriptionally silenced by X-chromosome inactivation which is linked to increased CpG island methylation and inactive heterochromatin marker such as the tri-methylated histone (H3K9me3) and changes in histone acetylation[9, 11, 21].

RBM10 regulates alternative splicing of various genes involved in apoptosis, cell proliferation, inflammation, and pathogenesis of viral infection[7, 22, 34, 56]. In addition, RBM10 has been implicated in cell invasion, metastasis and cell cycle revealing both

pro- and anti-tumour function of RBM10[13, 22, 27, 38]. Furthermore, loss-of-function mutation of RBM10 is associated with X-linked disorder TARP (talipes equinovarus, atrial septal defect, Robin sequence, and persistence of the left superior vena cava) syndrome and XLMR (X-linked mental retardation)[20, 33]. Moreover, RBM10 is frequently mutated in cancers including lung adenocarcinoma, renal cell carcinoma, thyroid cancer, hepatocellular carcinoma, and astroblastoma[4, 5, 22, 28, 32, 35, 48, 71, 74, 77, 78]. Moreover, RBM10 has also been implicated in drug resistance in acute myeloid leukemia[68]. Yet, the molecular mechanism as how these mutations affect RBM10 function in such diseases is still unclear. Recently, we showed that RBM10 interacts with a variant poly(A) polymerase Star-PAP and regulates 3′-end formation of target anti-hypertrophy gene expression indicating its role as a central regulator of heart failure[51]. Consequentially, RBM10 is down regulated during hypertrophy and heart failure in *in vivo* animal heart and *in vitro* myocyte hypertrophy model[51]. However, how RBM10 functions and/or its regulation is still unclear.

RBM10 is identified as a target of a proto-oncogene c-Src from a peptide array in a study to map global targets of cSrc with three putative target sites (Y-71, Y-500, T-971) [3]. Interestingly, cSrc is implicated in multiple cellular functions including cell proliferation, migration, and adhesion[2, 60]. In addition, cSrc is activated in response to pressure overload myocardial hypertrophy[17, 66]. Phosphorylation of cSrc kinase in the left ventricle of spontaneously hypertensive rats affects function of various target hypertrophic regulator[17]. However, how cSrc mediated phosphorylation of RBM10 affects RBM10 function or its anti-hypertrophy activity in the heart remains to be studied.

In order to understand how RBM10 anti-hypertrophy function is mediated, here, we analysed c-Src phosphorylation of RBM10 that is lost on mutation of the three cSrc target tyrosine (Y) residues to phenylalanine (F) (Y81F, Y500F and Y971F) or on inhibition/knockdown of c-Src. We showed that RBM10 phosphorylation is induced (while RBM10 expression is down regulated) in the isoproterenol-induced hypertrophic

heart consistent with activation of cSrc. Inhibition of cSrc kinase accentuated isoproterenol-induced hypertrophy and resulted in an early attainment of hypertrophy. Similar results were obtained in cellular model of hypertrophy in H9c2 cells. Interestingly, inhibition of ERK (that regulates RBM10 protein levels) prevented RBM10 down regulation and consistent attenuation of hypertrophic progression in both animal heart and cellular hypertrophy model. However, ERK inhibition did not show significant effect on hypertrophic progression in the presence of cSrc inhibition. Consistently, RBM10 re-expression after cSrc inhibition or re-expression of triple phosphomutant RBM10 failed to reverse cardiomyocyte hypertrophy. We demonstrated that RBM10 phosphorylation controls RBM10-Star-PAP interaction and its nuclear localisation to regulate target anti-hypertrophy gene expression in the heart. Our data establish that elevated RBM10 tyr phosphorylation by cSrc kinase drives RBM10 anti-hypertrophy function during hypertrophic induction in the heart.

OBJECTIVES

1. To characterize cSrc-mediated RBM10 phosphorylation events and its role in the regulation of hypertrophy gene program in the heart
2. To understand the significance of cSrc-mediated RBM10 phosphorylation in cardiac hypertrophy and progression to heart failure
3. To elucidate the molecular mechanism how RBM10 phosphorylation enables its cellular and physiological function in the heart.
4. To study upstream signaling events that regulates RBM10 phosphorylation and its implication in the downstream cellular events during hypertrophic induction

MATERIALS AND METHODS

Cell lines, animals, transfections and treatment

Human embryonic kidney (HEK293) and rat cardiomyoblast (H9c2) cells were obtained from American Type Culture Collection. Cells were cultured at 37°C in 5% CO_2 in high glucose Dulbecco's modified Eagle's medium (DMEM) supplemented with 10% fetal bovine serum and 50 IU/ml penicillin and streptomycin mix. siRNA oligos and plasmid DNA transfections were carried out using calcium phosphate method as described earlier[63]. Cells were then harvested 48-hr post-transfection for downstream RNA and protein analysis.

All animal experiments were approved by the Institutional Animal Ethics Committee (IAEC), and the guidelines prescribed for experiments using animal subjects were strictly followed. Eight- to twelve-week-old male Wistar rats were used for the experiment. Animals were procured and housed in a temperature and humidity controlled animal facility.

DNA Constructs:

FLAG- and His- tagged human RBM10 (RBM10 protein: NP_001191397.1, Transcript variant 5: NM_001204468.2) and rat RBM10 plasmid were as described earlier[51]. Phospho deficient mutations (Y81F, Y500F, Y971F, Y81F-500F, Y81F-500F-971F) were created using site directed mutagenesis of the tyrosine residues to phenylalanine as described previously[63]. Silence resistant mutations were generated in the RBM10 construct to render it insensitive to the siRNA oligos.

In vitro Kinase assay

In vitro kinase assays were carried out using immunopurified FLAG-tagged wild type or phosphomutant (individual or in combination) (Y81F, Y500F, Y971F, Y81F-500F, Y81F-500F-971F) RBM10 from HEK293 cells as described earlier[40]. Approximately 10 μg of FLAG-RBM10 (WT or mutants) were incubated with 10 μCi [γ32P] ATP in the

presence of 10 μg immunopurified kinases (CKIα, PKCδ or cSrc) in the kinase buffer (250 mM Tris-HCl, pH 7.5, 50 mM glycerol phosphate, 100 mM $MgCl_2$, 0.1 mM sodium vanadate, and 10 mM DTT) at 30°C for 1-hr as described previously [36]. Reactions were terminated by SDS sample dilution buffer and analysed on SDS-PAGE and detected by phosphor-imaging.

Protein Purification

Affinity purified human wild type FLAG-RBM10 and phosphomutant RBM10 was obtained from HEK293 cells after over expression of RBM10 pCMV Tag2A constructs. FLAG-epitope tagged proteins were then purified using FLAG M2 beads (Sigma) as described earlier[39]. Recombinant His-tagged RBM10 purifications were performed as described previously[50]. For purification of His-tagged RBM10 and corresponding mutants, the pET28 RBM10 constructs were used. His-tagged protein was obtained by over expression in *E. coli BL21(DE3)* after induction with 0.5 mM IPTG at 37°C for 4-hr or 18°C overnight. Tagged proteins were purified using Ni-NTA affinity chromatography as described previously[41]. Proteins were concentrated with poly ethylene glycol (PEG), snap frozen and stored at −80°C.

Phosphoamino acid analysis by one-directional TLC

Recombinant wild type His-RBM10 or phosphomutants after in vitro kinase reaction using purified cSrc kinase was hydrolysed with 10X volume of 6 N HCl at 110°C for 1-hr as described earlier[18]. Samples were separated on a TLC buffer system (5:2:1 butanol: formic acid: water) until it migrated to the top edge of the TLC plate and sprayed with 0.1% solution of ninhydrin in acetone (for standard amino acids) before analysis on a phosphor-screen for radiolabelled hydrolysed amino acids. Alongside, an equivalent amount of hydrolysed standard phosphoamino acids (phosphotyrosine or phosphoserine, 1 μg each) were analysed on the same plate.

Immunoprecipitation and Immunoblotting

Immunoprecipitations and immunoblottings from cell lysates were carried out as described earlier[44]. Input = 10% of the total protein used for IP. For immunoprecipitation from rat heart, tissues were lysed in IP buffer (100 mM KCl, 50 mM Tris-HCl pH 7.4, 5 mM EDTA, 0.5% Nonidet NP-40, 100 μg/ml RNase A, 200 mM $NaVO_4$, 50 mM L-glycerophosphate, 50 mM NaF and 1 × EDTA-free protease inhibitor cocktail (Roche) with gentle sonication (amplitude= 28%, 5 sec on/5 sec off for 5 minutes).

3′-RACE Assay and 3′-end cleavage measurement

Total RNA was isolated from H9c2, HEK293 cells, and animal tissues using RNAeasy mini Kit (Qiagen). 3′-RACE assays were carried out as described earlier[52]. RACE products were confirmed by sequencing. For measurement of cleavage efficacy, uncleaved mRNA levels were measured by quantitative real time PCR (qRT-PCR) using a pair of primers across the cleavage site as described earlier [52]. The non-cleaved RNAs were expressed as fold-change over total mRNA after normalising with internal control GAPDH levels.

Hypertrophy induction in H9c2 cell line and Wistar rat heart

Eight- to twelve-week-old rats were administered isoproterenol (15 mg/kg animal body weight) intraperitoneally for 7 consecutive days, whereas control animals were given normal saline as described previously[51]. Rats were then sacrificed after assessment of echocardiogram for cardiac hypertrophy followed by analysis of heart weight, cross-section, luminal space, and various molecular markers of hypertrophy.

In the case of the H9c2 cell line, cells were grown to 60% confluency and treated with 100 μM isoproterenol in DMSO for 48-hr. Chemically induced hypertrophy was tested

with molecular markers (Western blotting and qRT-PCR) and changes in cell size and morphology (IF imaging). For rescue experiments with RBM10 re-expression, cells were transfected with the rat RBM10 construct 48-hr after knockdown.

cSrc and ERK Kinase inhibition in animal and H9c2 cells

Eight- to twelve-week-old rats were administered isoproterenol (15 mg/kg animal body weight) intraperitoneally for 7 consecutive days along with ERK inhibitor (SCH 772984) and cSrc inhibitor (PP2) as required at a concentration of 1 mg/kg and 1.5 mg/kg respectively as described previously[43]. Another tyrosine kinase inhibitor (SU6668) was injected intraperitoneally at a concentration of 1 mg/kg in the control inhibitor group. Rats were then subjected for analysis of hemodynamic parameters using echocardiography and sacrificed for left ventricular heart tissue sample which was then used for testing molecular markers (qRT-PCR and western blotting) and imaging.

In vitro cellular hypertrophy assay

To test the cellular and molecular changes during hypertrophy, H9c2 cells were treated with hypertrophy agonist isoproterenol (100 μM in DMSO) for 48-hrs[67]. Knockdown or expression of RBM10 was carried out as described above[63]. For rescue experiments with RBM10 re-expression, cells were transfected with rat RBM10 construct 48-hr post knockdown. Molecular changes after the treatment or knockdown were analysed by qRT-PCR (from RNA isolated from the cells) or Western blotting after cells were lysed in SDS lysis buffer. For IF imaging, cells were seeded onto collagen-coated coverslips, fixed in 4% PFA, stained with Phalloidin and DAPI and prepared for IF as described above.

Real-Time qPCR

Real-time qPCR was carried out in a CFX98 multi-color system (Bio-Rad) using SYBR Green Supermix using 2 μg total RNA reverse-transcribed with MMLV-RT (Invitrogen) as described earlier [52]. Single-product amplification was confirmed by melting curve analysis, and primer efficiency was near 100% in all experiments. Quantifications were expressed in arbitrary units, and target mRNA abundance was normalised to the expression of GAPDH with Pfaffl method[55]. All real-time qPCR results were representative of at least three independent experiments ($n > 3$). For real-time qPCR of animal tissues, at least 5 animals were used ($p < 0.05$).

Immunofluorescence assay

IF experiments were carried out as described previously[50]. Briefly, H9c2 and HEK293 cells were rinsed with PBS and fixed in 4% paraformaldehyde for 15 minutes. Following fixation, cells were permeabilised using 0.1% Triton-X 100 for 15 minutes, followed by blocking with 3% BSA for 30 minutes. Cells were then incubated with primary antibody specific for RBM10 (Thermo) at 4°C overnight. Next day, cells were incubated in secondary antibody Alexa 488 (Invitrogen) against the Rabbit IgG. The actin filaments and nucleus were counterstained with Phalloidin (Sigma) and DAPI respectively. Images were captured using confocal microscopy. Z stacked images were taken to obtain details of images in all planes (Olympus, Japan) and images were finally analysed using Olympus Cell Sens software.

Immunohistochemistry

Immunohistochemistry was carried out using formalin-fixed, paraffin-embedded heart ventricle tissue sections from control and test groups as described earlier[47]. Tissue sections were de-paraffinised in xylene and rehydrated using different grades of alcohol. This was followed by antigen retrieval by incubating in 10 mM Sodium citrate at 95°C for 30 minutes followed by quick cooling on ice. Tissue sections were then blocked

in 3% BSA for 30 minutes and incubated with primary antibody for RBM10 at 4°C overnight. Next day, tissue sections were washed in TBS-T (Tris buffered saline -Tween 20) and incubated with Rabbit secondary IgG tagged with Alexa 571 (Invitrogen) at room temperature for 1-hr. Antibody bound tissue sections were then counterstained with DAPI to stain nucleus and mounted using Flour mount (Sigma). Imaging was performed using confocal microscope (Olympus, Japan).

Preparation of nuclear, cytoplasmic and total cell fraction

Nuclear fractions from both cell line and tissues were prepared using NE-PER nuclear extraction kit (Thermo Scientific) as described earlier[39]. 95% confluent cell culture 10cm dish and 40 mg of heart tissue samples were used to extract nucleus. All steps were done according to manufacturer's instruction. In case of animal tissue, initial lysis of tissue sample was carried out in liquid nitrogen using a mortar and pestle and then dissolved in lysis buffer (20 mM HEPES, 350 mM NaCl, 350 mM, 20% Glycerol, 1% NP-40, 1 mM $MgCl_2$, 0.5 mM EDTA, 0.1 mM EGTA, 0.5 mM DTT and PI tablet). Nuclear, cytoplasmic and total fractions were tested with respective marker proteins.

Statistics

All data were obtained from at least three independent experiments and are reported as mean ± SEM. The statistical significance of the differences in the mean was calculated using ANOVA. The differences were considered statistically significant at a p value of less than 0.05.

RESULTS

1. RBM10 is phosphorylated at three tyrosine residues by proto-oncogene cSrc kinase

RBM10 (NP_001191397.1) was earlier shown as a target of tyrosine kinase cSrc from a global cSrc target peptide microarray followed by mass spectrometry sequencing[3]. Analysis showed three putative cSrc phosphorylation sites - Y81 in the RRM1 motif, Y-500 in the OCRE domain, and Y-971 in the G-patch domain (**Fig. 1A**). To validate this phosphorylation, we first performed in vitro kinase assay of recombinant His-RBM10 using immunopurified cSrc kinase. We observed kinase activity of cSrc but not of control kinases CKIα or PKCδ on RBM10 (**Fig. 1B**). Immunoprecipitation experiment from HEK293 cell lysate also indicated cSrc kinase association with RBM10 (**Fig. 1C**). To further assess the cSrc target phosphorylation sites, we mutated the three-tyrosine phosphorylation residues to phenylalanine to generate phospho-deficient mutations[18] individually and in combination (Y81F, Y500F, Y971F, Y81F-500F, Y81F-500F-971F). Next, we carried out *in vitro* kinase assay of recombinant RBM10 mutants along with wild type RBM10 using immunopurfied cSrc from the cell as described earlier[40]. We observed kinase activity on the wild type RBM10 that was lost on mutation of the three-tyrosine residues to phenylalanine (triple phospho-mutation) (**Fig. 1D**). While individual amino acid mutations showed a modest reduction in the phosphorylation, increasing number of tyrosine to phenylalanine mutations resulted in a gradual decrease in the phosphorylation of RBM10 (**Fig. 1D**).

To confirm RBM10 tyrosine phosphorylation by cSrc, we carried out direct phosphoamino acid analysis on ^{32}P-radiolabelled RBM10 after *in vitro* phosphorylation with cSrc kinase. Acid hydrolysed ^{32}P-radiolabelled RBM10 was then analysed on a one directional Thin Layer Chromatography (TLC)[18]. The migration of the radiolabelled amino acid residue observed on the TLC after acid hydrolysis was equivalent to that of phosphotyrosine standard but not of phosphoserine standard revealing that RBM10 is phosphorylated at the tyrosine residue (**Fig. 1E**). Consistently, triple phospho-mutation (Y81F-500F-971F) of RBM10 resulted in the loss of phospho-tyrosine detection on TLC after RBM10 acid hydrolysis. Whereas there was no significant effect of individual phosphorylation site mutations (Y81F, Y500F, Y971F) on the phospho-tyrosine detection

(**Fig. 1E**). Together, these results indicate that RBM10 is phosphorylated by cSrc kinase at the three-tyrosine residues Y81, Y500 and Y971.

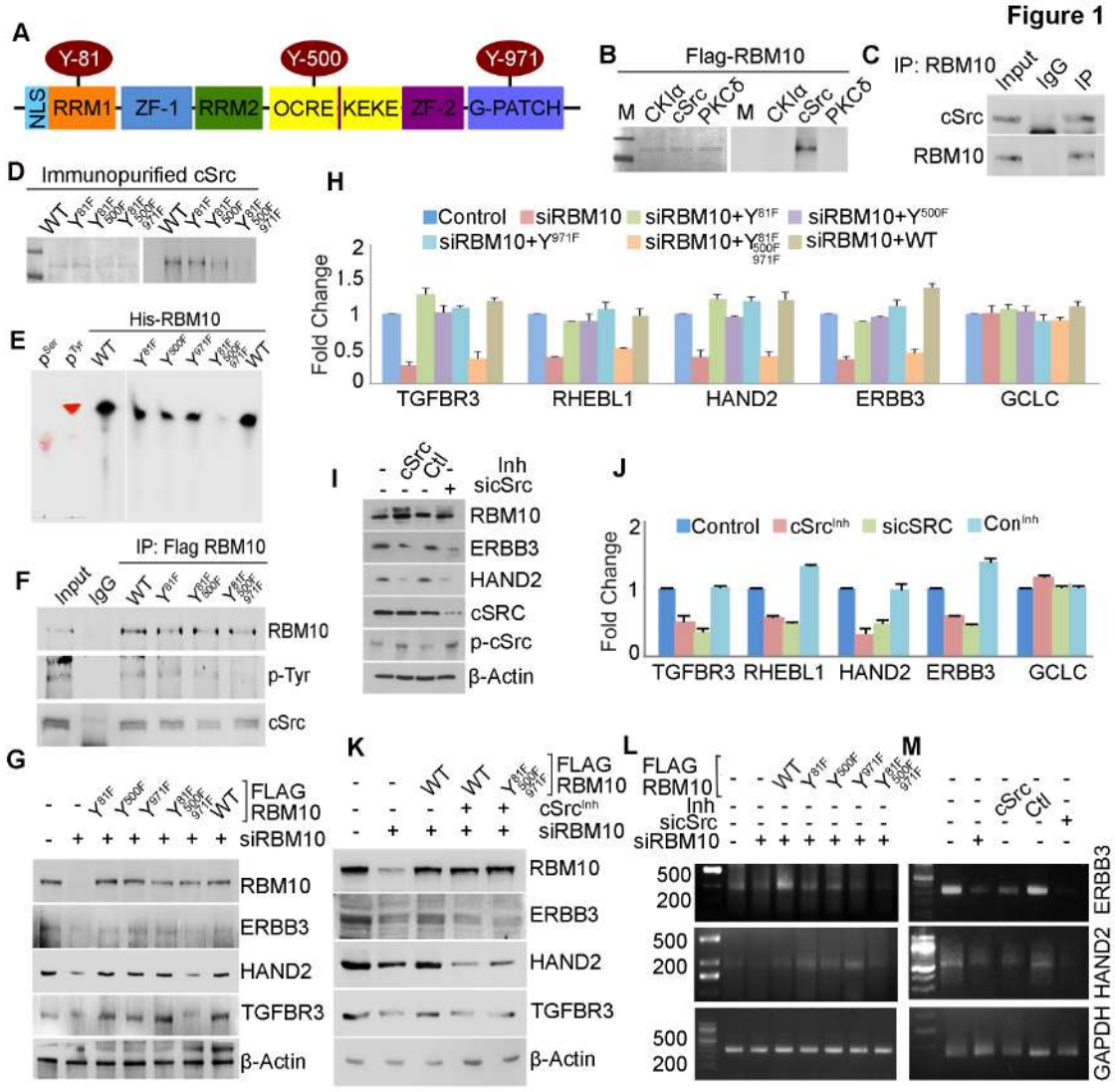

Fig. 1: RBM10 is phosphorylated by proto-oncogene cSrc tyrosine kinase at 3 different tyrosine residues. **(A)** Schematics of RBM10 domain architecture depicting location of 3 cSrc targeted phosphorylation sites - tyrosine 81, 500 and 971 residues (Y-81, Y-500, Y-971) at different domains of RBM10. Sequence around each tyrosine phosphorylation site is shown in the Supplementary Fig. 1A. **(B)** In vitro kinase assay of

anti-FLAG affinity purified RBM10 from HEK293 using immuno-purified kinases CKIα, cSrc and PKCδ (right panel). Coomassie stained gel images of same proteins are represented at the left panel. **(C)** Immunoblotting analysis of cSrc protein after immunoprecipitation with antibodies specific to RBM10 and control IgG from HEK293 cells. Input = 10% of the IP lysate. (**D**) In vitro kinase assay of anti-FLAG affinity purified wild type and different phosphomutant RBM10 [tyrosine 81 to phenylalanine (Y-81F), tyrosine 81 and 500 to phenylalanine (Y81F-500F), and triple phospho-mutation (tyrosine 81, 500 and 971 to phenylalanine (Y81F-500F-971F)] using immuno purified cSrc kinase (right panel). Coomassie stained images of proteins are represented on the left panel. **(E)** Direct phosphoamino acid analysis using one directional TLC after acid hydrolysis of in vitro phosphorylated wild-type RBM10 and corresponding individual and triple-phospho mutant RBM10 (Y-81F, Y-500F, Y-971F, and Y81F-500F-971F). Ninhydrin stained control phospho-tyrosine and -serine amino acids are shown at the left. **(F)** Immunoblotting with antibodies specific to cSrc, phospho-tyrosine and RBM10 after immunoprecipitaion with FLAG-RBM10 and control IgG from HEK293 cells expressing wild type FLAG-epitope tagged RBM10 and its respective phosphomutants as indicated. Input = 10% of the IP lysate. **(G)** Immunoblotting analysis of RBM10, target proteins (HAND2, TGFBR3 and ERBB3), and control β-Actin from HEK293 cells after knockdown of RBM10 and rescue with wild type RBM10 and respective individual and triple phopsho-mutant (Y81F, Y500F, Y971F, and Y81F-500F-971F) that are insensitive to siRNA used for the knockdown as indicated. **(H)** qRT-PCR analysis of RBM10 target mRNAs (*TGFBR3*, *RHEBL1*, *HAND2*, *ERBB3* and non target control *GCLC*) from total RNA isolated from HEK293 cells after siRNA knockdown of RBM10 and rescue with wild type RBM10 and different phosphomutants as in G. Error bar represents standard error mean (SEM) of n=3 independent experiments. [p values (<0.02 in siRBM10 and siRBM10 rescued with triple phopsho-mutant (Y81F-500F-971F) RBM10 for *TGFBR3*), (<0.01 in siRBM10 and siRBM10 rescued with triple phopsho-mutant for *RHEBL1*), (<0.04 in siRBM10 and 0.03 in rescued with triple phopsho-mutant for *HAND2*), and (<0.04 in siRBM10 and 0.02 in siRBM10 rescued with triple phopsho-mutant for *ERBB3*); siRBM10 rescue with Y81F, Y500F, Y971F individual mutations and wild type (WT) RBM10 values did not show significant difference relative to control for all genes]. (**I**) Immunoblotting analysis of RBM10, cSrc, p-cSrc and RBM10 target proteins (HAND2 and ERBB3) from HEK293 after treatment with cSrc inhibitor, control tyrosine kinase inhibitor, and/or transfection with siRNA specific for cSrc kinase. (-) siRNA indicates that control scrambled RNAi was used. **(J)** qRT-PCR analysis of RBM10 target mRNAs as indicated and non-target control *GCLC* from total RNA isolated from HEK293 cells under the same conditions as in I. Error bar represents standard error mean (SEM) of n=3 independent experiments. [p values (<0.01 in cSrc inhibitor treatment ($cSrc^{Inh}$) and siRNA cSrc depletion for *TGFBR3*), (<0.04 in $cSrc^{Inh}$ and 0.001 in sicSrc for *RHEBL1*), (<0.03 in $cSrc^{Inh}$ and 0.01 in sicSrc for *HAND2*), and (<0.01 in both $cSrc^{Inh}$ and sicSrc for *ERBB3*); Control inhibitor (Ctl^{Inh}) treatment values did not show significant difference relative to control for all genes]. (**K**) Immunoblotting analysis of RBM10 target proteins (HAND2, TGFBR3, ERBB3) from HEK293 cells after siRNA knockdown of RBM10 and rescue with wild type and triple-phospho mutant RBM10 in the presence and absence of cSrc inhibition. (**L-M**) 3'-RACE assay of RBM10 target mRNAs (*HAND2*, *ERBB3*) and control *GAPDH* from HEK293 cells under the conditions as indicated.

Next, to confirm cSrc phosphorylation of RBM10, we FLAG affinity purified RBM10 from cells expressing FLAG-RBM10 bearing the tyrosine to phenylalanine mutations as described above. Purified FLAG-RBM10 was examined for tyrosine phosphorylation using phospho-tyrosine specific antibody. Consistent with our *in vitro* results, we detected phospho-tyrosine from the purified wild type RBM10 that was lost on triple phospho-mutation (Y81F-500F-971F) in Western blot analysis (**Fig. 1F**). We also saw similar decrease in the intensity of phosphotyrosine RBM10 band in the immunoblot with increase in the number of tyrosine to phenylalanine mutations (**Fig. 1F**). Together these results confirm that RBM10 is phosphorylated at the three-tyrosine residues (Y81, Y500, and Y971) by cSrc tyrosine protein kinase.

2. cSrc-mediated RBM10 phosphorylation controls expression and 3′-end processing of target mRNAs

To further determine the significance of RBM10 tyrosine phosphorylation, we assessed target anti-hypertrophy gene expression by qRT-PCR and Western blot analysis after cSrc inhibition and/or by knockdown/rescue approach. Some of the key antihypertrophy regulators like *HAND2*, *ERBB3*, *RHEBL1*, TGFBR3 are regulated by RBM10, they require the assembly of Star-PAP polyadenylation machinery at the 3′- end of the RNA[51]. We observed consistent loss of protein expression (HAND2, ERBB3, TGFBR3) on RBM10 knockdown that was rescued by ectopic wild type RBM10 re-expression (**Fig. 1G**). However, RBM10 triple phospho-mutation failed to rescue the expression of the target proteins (**Fig. 1G**). Nevertheless, individual phospho-mutations rescued the target gene expression similar to the wild type RBM10 (**Fig. 1G**). qRT-PCR analysis also showed loss of target mRNA expression (*HAND2*, *ERBB3*, *RHEBL1*, *TGFBR3*) on RBM10 knockdown that was rescued by wild type RBM10 or individual phospho-mutations but not by the triple phospho-mutation (**Fig. 1H**). Similarly, treatment with cSrc inhibitor (PP2) but not the control tyrosine kinase inhibitor (SU6668) and siRNA specific depletion of cSrc resulted in the loss of both target protein and mRNA

expression (**Fig. 1I, 1J**). Strikingly, wild type RBM10 failed to rescue loss of target mRNA and protein expressions on RBM10 knockdown after inhibition of cSrc (**Fig. 1K**). Moreover, cSrc inhibition did not have further effect on the expression of target mRNA and protein levels after triple phospho-mutation on RBM10 (**Fig. 1K**). Together, these results indicate that RBM10 phosphorylation at the three Tyr residues (Y81, Y500 and Y971) is required for RBM10 target gene expression.

Since RBM10 regulates 3′-end processing of mRNAs along with Star-PAP, we analysed the 3′-end formation of target mRNAs (*HAND2*, *ERBB3*) by 3′-RACE[52]. Consistent with qRT-PCR results, we saw loss of 3′-RACE product after RBM10 knockdown that was rescued by wild type RBM10 but not by the triple phospho-mutant RBM10 (**Fig. 1L**). Individual mutations behaved similar to that of wild type and did not significantly affect the 3′-end formation of target mRNAs (**Fig. 1L**). Similarly, cSrc inhibition or knockdown resulted in the loss of 3′-end formation similar to RBM10 depletion (**Fig. 1M**). These results were also corroborated in cleavage assays. Together, these results reveal that RBM10 phosphorylation by cSrc at the three tyrosine residues regulate target pre-mRNA 3′-end processing and mRNA expression.

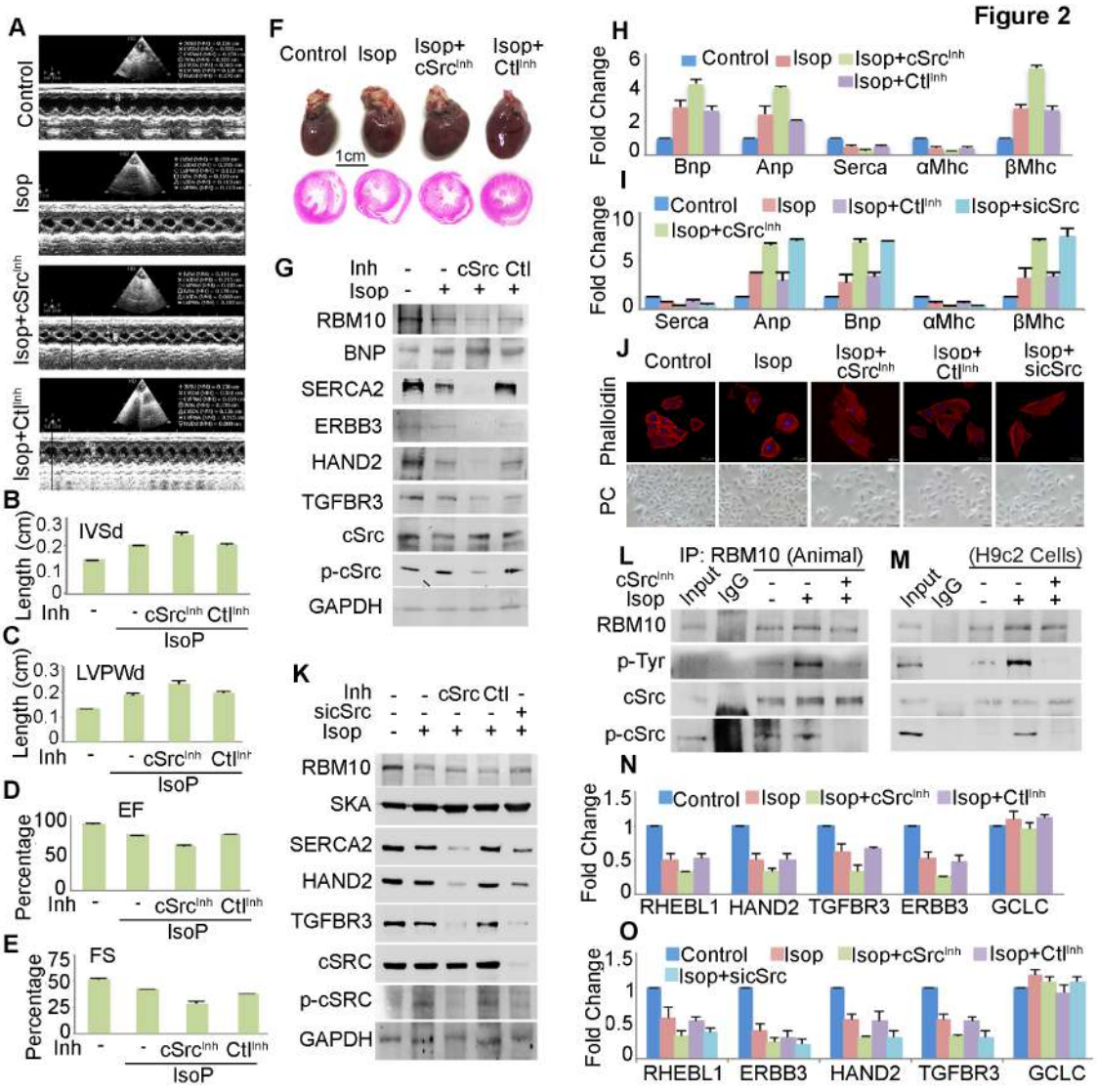

Fig. 2: cSrc-mediated RBM10 phosphorylation is induced during cardiac hypertrophy and regulates target anti-hypertrophy gene expression. (**A**) Echocardiogrm of control and isoproterenol induced hypertrophic animal heart in the presence and absence of cSrc and control tyrosine kinase inhibitor treatment as indicated. (**B-C**) Measurement of interventricular septum diastole (IVSd) and left ventricular posterior wall thickness (LVPWd) of hearts from the echocardiography of control and hypertrophic animals in A. (Error bar represents SEM from n = 5 per group, p values <0.001 in isoproterenol treatment, <0.003 in isoproterenol treatment in the presence of cSrc inhibition and control inhibitor treatment relative to control animal heart for IVSd; and <0.002 in isoproterenol, isoproterenol+cSrc-inhibition and isoproterenol+control inhibitor treatment for LVPWd). (**D-E**) Measurement of left

ventricular ejection fraction (LVEF %) and left ventricular fraction shortening (LVFS %) of control and hypertrophic heart as in A (Error bar represents SEM from n = 5 per group, p values <0.001 in all three conditions isoproterenol, isoproterenol+cSrc-inhibition and isoproterenol+control inhibitor for both LVEF and LVFS). (**F**) Comparison of heart sizes and cross section of control versus hypertrophic heart as in A. (**G**) Western blot analysis of RBM10, target proteins (HAND2, TGFBR3), hypertrophic markers (SERCA2A, BNP), cSrc and activated cSrc from control rat heart and isoproterenol induced hypertrophic rat heart in the presence and absence of cSrc or control inhibitor treatment. Each blot is representative of n=3 independent blotting experiments. (**H**) qRT-PCR analysis of mRNA levels of various hypertrophy markers as indicated from total RNA isolated from heart tissues under the same conditions as in G. Error bar represents standard error mean (SEM) of n=3 independent experiments. [p values (<0.05 in isoproterenol, isoproterenol+ $cSrc^{Inh}$ and isoproterenol+ Ctl^{Inh} for *BNP* and *ANP*), (<0.01 in isoproterenol, isoproterenol+ $cSrc^{Inh}$ and isoproterenol+ Ctl^{Inh} for *SERCA2A* and *α-MHC*), and (<0.01 isoproterenol, isoproterenol+ $cSrc^{Inh}$ and isoproterenol+ Ctl^{Inh} for *β-MHC*) relative to control. **(I)** qRT-PCR analysis of mRNA levels of various hypertrophy markers as indicated from total RNA isolated from H9c2 cell line after isoproterenol treatment in the presence and absence of cSrc or control tyrosine kinase inhibitor. Error bar represents standard error mean (SEM) of n=3 independent experiments. [p values (<0.04 for *SERCA2A* and *ANP* in all conditions), (<0.03 for *β-MHC, BNP* and *α-MHC*) relative to control. **(J)** Phase contrasts (PC) and IF imaging of phalloidin stained H9c2 cells after treatment with isoproterenol in the presence and the absence of cSrc or control inhibitor as indicated. Quantification of the cell surface area is shown in Supplementary Fig. 2E. **(K)** Western blot analysis of various hypertrophic markers, RBM10, and its target proteins after induction of hypertrophy in H9c2 cell line by isoproterenol treatment in the presence and absence of cSrc or control tyrosine kinase inhibitor treatment as indicated. Each blot is representative of n = 3 independent experiments. (**L**) Immunoprecipitation experiment of RBM10 from control and hypertrophic heart tissues in the presence and absence of cSrc inhibition followed by Western blot analysis of RBM10, phosphorylated RBM10 and cSrc as indicated. Input = 10% of the IP lysate. (**M**) Immunoprecipitation of RBM10 from H9c2 cells after treatment with isoproterenol in the presence and absence of cSrc inhibition followed by Western blot analysis as in L. Input = 10% of the IP lysate. (**N**) qRT-PCR analysis of mRNA levels of various RBM10 targets as indicated from total RNA isolated from heart tissues under the same conditions as in H. Error bar represents standard error mean (SEM) of n=3 independent experiments. [p values (<0.009 for *RHEBL1* and *HAND2* in all conditions), (<0.04 for *ERBB3,* and *TGFBR3* in all conditions) relative to control. (**O**) qRT-PCR analysis of mRNA levels of various RBM10 targets as indicated from total RNA isolated from H9c2 cell line after isoproterenol treatment in the presence and absence of cSrc or control tyrosine kinase inhibitor. Error bar represents standard error mean (SEM) of n=3 independent experiments. [p values (<0.01 for *RHEBL1, HAND2,* and *ERBB3* in all conditions), (<0.03 for *TGFBR3* in all conditions) relative to control.

3. cSrc-mediated RBM10 phosphorylation is induced during hypertrophy in both cellular and animal heart model of hypertrophy

To determine the significance of cSrc-mediated RBM10 phosphorylation, we

employed the chemical (isoproterenol) induced Wistar rat heart model of cardiac hypertrophy [57] in the presence and absence of cSrc inhibition[43]. We also used cellular hypertrophy model in H9c2 cells[67] in the presence and absence of cSrc inhibition or knockdown[43]. In our animal model, hypertrophy was induced in the Wistar rat heart by intra-peritoneal isoproterenol injection for one week and monitored after heart transitioned into hypertrophic state. Induced-hypertrophy was assessed by analysis of structural and hemodynamic parameters of the heart by echocardiography such as diastolic inter ventricular septal dimension (IVSd), diastolic left ventricular posterior wall thickness (LVPWd), left ventricular ejection fractions (LVEF), and left ventricular fractional shortening (LVFS) [61] (**Fig. 2A-F**)**.** This was further confirmed by measuring levels of molecular markers of hypertrophy from the heart tissue after animal was sacrificed (**Fig. 2G-H**) [16, 42]. Echocardiogram of hypertrophic animal heart showed increased IVSd and LVPWd, and a decrease in LVEF and LVFS measures in isoproterenol-injected animals confirming hypertrophic state of the animal heart (**Fig. 2A-E**). There was an enhancement in the heart size with a concomitant increase in relative heart mass, and ventricular wall thickness and increased total protein content of isoproterenol-injected animal heart compared to the control animals (**Fig. 2F**). In Western blot analysis, we found reduction in the protein level of molecular marker SERCA2A whereas there was an increase in the level of another molecular marker BNP (**Fig. 2G**). Moreover, we observed increased expression of *ANP, BNP*, and *β-MHC,* and a reduction in the expression of *SERCA2A* and *α-MHC* mRNA in qRT-PCR analysis from the hypertrophic heart tissue (**Fig. 2H**). Similarly, in H9c2 cells, hypertrophy was confirmed by assessing cellular and molecular changes (**Fig. 2I-K**). As in the case of animal heart, there were differential changes in the molecular makers on isoproterenol treatment in both qRT-PCR analysis (increased *ANP, BNP*, and *β-MHC,* and a reduction in *SERCA2A*, and *α-MHC*) and Western blot (reduction in SERCA2A and increase in SKA) in H9c2 cells (**Fig. 2I, 2K**). Moreover, we also observed increased cell surface area and actin filament reorganisation in the immunofluorescence analysis of isoproterenol treated H9c2 cells confirming hypertrophic state of the myoblast cells (**Fig. 2J).**

RBM10 is down regulated during hypertrophy that resulted in the reduced expression of target mRNAs[51]. Consistently, we observed RBM10 down regulation both *in vivo* hypertrophic heart and *in vitro* H9c2 cells after isoproterenol treatment (**Fig. 2G, 2K**). To assess status of RBM10 phosphorylation in hypertrophic myocyte, we immunoprecipitated RBM10 from both hypertrophic rat heart tissue and H9c2 cell, and analysed with phospho-tyrosine antibody in Western blot experiment. We observed induced RBM10 tyrosine phosphorylation (>3-fold increase) on hypertrophy induction in both cellular and animal heart models (**Fig. 2L-M**). However, the induction in the RBM10 phosphorylation on isoproterenol treatment was diminished on cSrc inhibition. We saw cSrc activation in both hypertrophic myocyte and animal heart tissue congruent with induced RBM10 tyrosine phosphorylation (**Fig. 2G, 2K-M**). Similar loss of phosphorylation was seen on siRNA cSrc depletion but not control siRNA treatment or control tyrosine kinase inhibition in H9c2 cells on isoproterenol treatment (**Fig. 2K**). Therefore, we infer that cSrc activation in hypertrophic myocytes induces RBM10 phosphorylation.

4. cSrc-mediated RBM10 phosphorylation controls anti-hypertrophy gene expression and enables anti-hypertrophy function in the heart

In the animal hypertrophy heart model, while we found increase in LVPWd and IVSd, and a similar decrease in LVFS or LVEF, cSrc inhibition led to a further accentuation of hemodynamic and molecular hypertrophic parameters tested (**Fig. 2B-H**). There was >20% increase in the LVPWd and IVSd, whereas >30% decrease in LVFS or LVEF on cSrc inhibition compared to that of isoproterenol treated animal heart (**Fig. 2B-E**). Moreover, similar augmentation in the changes was seen in the levels molecular markers tested in both qRT-PCR and Western analysis (**Fig. 2G-H**). There was further increase of 1.5 to 2-fold in the expression of *ANP*, *BNP*, and *SKA* and >20% reduction in the expression of *SERCA2A* and *α-MHC* on cSrc inhibition from that of isoproterenol

treatment (**Fig. 2G-H**). However, there was no difference in the expression of RBM10 in the presence of isoproterenol treatment on cSrc inhibition (**Fig. 2G**). Similarly, in the cellular hypertrophy model in H9c2, we observed a 3-fold increase in the cell size on isoproterenol treatment that was further raised to 6-fold after cSrc inhibition (**Fig. 2J**). Moreover, augmented expression of molecular markers were found in both Western (increase SKA and decrease SERCA2A) and qRT-PCR analysis increased *ANP, BNP*, and *β-MHC,* and a reduction in *SERCA2A*, and *α-MHC*) (**Fig. 2I, 2K**). Together, these results show that RBM10 phosphorylation regulates anti-hypertrophy function during myocyte hypertrophy.

To ascertain the effect of phosphorylation on RBM10 anti-hypertrophy function, we analysed RBM10 target mRNA and protein expression in the isoproterenol induced hypertrophic heart and cellular H9c2 models. We observed a reduction in mRNA and protein levels of RBM10 target genes in both *in vivo* hypertrophic heart models and *in vitro* cellular hypertrophy models (**Fig. 2N-O**). There was a marked reduction in the expression of target protein (ERBB3, HAND2) in Western and mRNAs (*RHEBL1*, *HAND2*, *ERBB3*, *TGFBR3*) in the presence of cSrc inhibition as observed by qRT-PCR analysis on isoproterenol-administered animal heart (**Fig. 2G, N**). Similarly, in the cellular model of hypertrophy, expression of target mRNAs and proteins were further accentuated on cSrc inhibition or on cSrc knockdown after isoproterenol treatment (**Fig. 2K, O**). Together, these results demonstrate that cSrc-mediated RBM10 phosphorylation mediates target anti-hypertrophy gene expression, which consequently regulates molecular and cellular changes in myocyte hypertrophy.

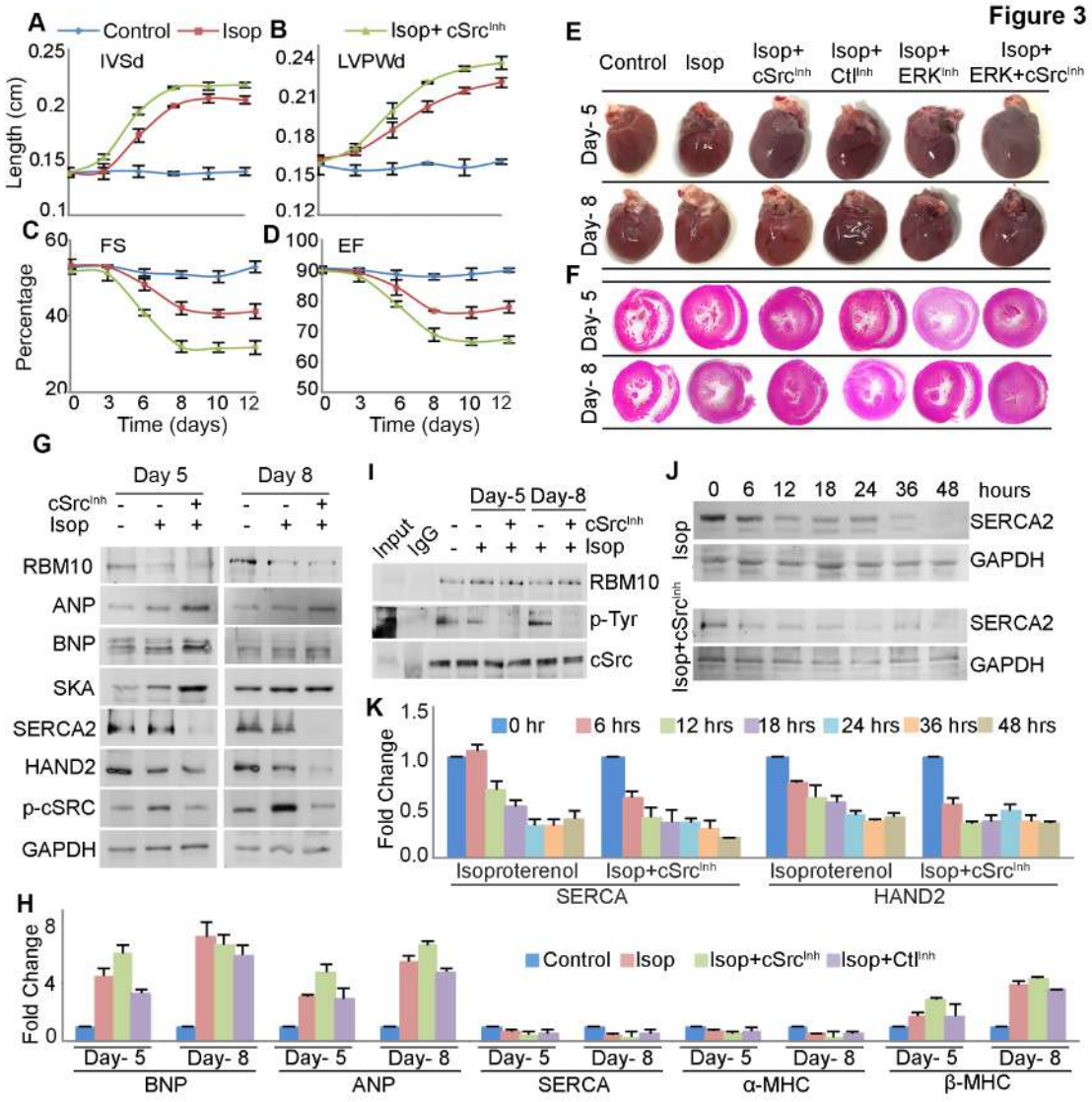

Fig. 3: cSrc-inhibition accentuates isoproterenol-induced hypertrophy in both animal heart and in vitro myocyte. (**A-B**) Measurement of interventricular septum diastole (IVSd) and left ventricular posterior wall thickness (LVPWd) of control and hypertrophic animals in the presence and absence of cSrc inhibition at various time points (from day 0 to day 12) post isoproterenol administration. Error bar represents SEM of n=5 animals per group. (**C-D**) Measurement of left ventricular ejection fraction (LVEF %) and left ventricular fraction shortening (LVFS %) of control and hypertrophic animals as in A. Error bar represents SEM of n=5 animals per group. (**E-F**) Comparison of the heart size and the cross section of control versus hypertrophic heart under the conditions as indicated, n=5 animals were taken per group. (**G**) Western blot analysis of

RBM10, target proteins and hypertrophic markers from day 5 and day 8 isoproterenol-induced hypertrophic heart in the presence and absence of cSrc inhibition as indicated. Control GAPDH is shown below. Each blot is representative of n=3 independent experiments. (**H**) qRT-PCR analysis of mRNA levels of various hypertrophic markers from total RNA isolated from control and hypertrophic heart tissues of day 5 and day 8 post isoproterenol administration in the presence of cSrc or control inhibitor as indicated. Error bar represents standard error mean (SEM) of n=3 independent experiments. [p values (<0.01 in day 5 and 0.02 in day 8 for *BNP* and *ANP* in all conditions), (<0.009 and 0.008 for *β-MHC* in day 5 and day 8, and (<0.02 in day 5 and 0.009 in day 8 for *SERCA2A* and *α-MHC* in all conditions)] relative to control. (**I**) Immunoprecipitation of RBM10 from control and hypertrophic heart under conditions as indicated followed by Western analysis with RBM10, phospho-tyrosine and cSrc specific antibodies. Input represents 10% of the IP sample. (**J**) Western blot analysis of hypertrophic marker SERCA2A from H9c2 cells after treatment with isoproterenol at various time points as indicated in the presence and absence of cSrc inhibition. (**K**) qRT-PCR analysis of mRNA levels of *SERCA2A* under the same conditions as in J. Error bar represents SEM of n=3 independent experiments. [p values (<0.009 in 18 to 48-hrs timepoints for isoproterenol treatment, and <0.05 for isoproterenol + $cSrc^{Inh}$ from 12-hrs to 48-hrs time points) relative to 0-hr time point. 6 and 12-hr time points for isoproterenol treatment and 6-hr time points for isoproterenol + $cSrc^{Inh}$ values did not show significant difference relative to 0-hr time points.

5. cSrc-inhibition accentuates isoproterenol induced-hypertrophy in both animal heart and in vitro myocyte

To understand the implication of cSrc-mediated RBM10 phosphorylation in cardiac hypertrophy, we administered isoproterenol and monitored the animal heart at various time points till heart turned hypertrophic. We assessed ventricular and hemodynamic parameters (IVSd, LVPWD, LVEF and LVFS) at different time points (day 0 to 12) in the presence and absence of cSrc inhibition (**Fig. 3A-D**). We observed sigmoidal increase in the ventricular muscle (wall) thickness (both IVSd and LVPWd) and similar decrease in the heart function (LVEF and LVFS) with increasing number of days post isoproterenol administration (**Fig. 3A-D**). There was a gradual and higher increase (in both IVSd and LVPWd) and a similar decrease (in LVEF and LVFS) up to day 8 from day 0 control animals. There were no marked changes in both ventricular and hemodynamic parameters after day 8 when animal heart was already hypertrophic. Strikingly, we observed significant accentuation of all four parameters of hypertrophy

assessed (IVSd, LVPWd, LVEF and LVFS) on cSrc inhibition. There was further 20-30% increase in the IVSd and LVPWd on cSrc inhibition from that of isoproterenol administered animal heart (**Fig. 3A-B**). Likewise, the accentuated decrease in LVEF and LVFS on cSrc inhibition from that of isoproterenol administration was around 40-50% (**Fig. 3C-D**).

Closer look of the hypertrophic heart (day 8 of isoproterenol administration) showed further induction in heart size and ~15% increase in the heart weight in addition to enhancement in IVSd, LVPWd or lowering in LVEF and LVFS on cSrc inhibition (**Fig. 3E-F**). Similar accentuations were visible in the animal heart day 5 post isoproterenol administration (**Fig. 3E-H**). In line with this finding, we saw additional reduction in the expression of molecular marker SERCA2A and increase in the ANP, BNP, and SKA in Western blot in hypertrophic heart in the presence of cSrc inhibition in both day 5 and day 8 treated animal hearts (**Fig. 3G**). Similarly qRT-PCR analysis also revealed heightening in the expression of *ANP*, *BNP*, *β-MHC* and further down regulation of *SERCA2A* and *α-MHC* mRNA on cSrc inhibited animal hearts treated with isoproterenol for day 5 and day 8 (**Fig. 3H**). Similarly, we observed a similar deepened down regulation of RBM10 targets gene expression in both mRNA (*RHEBL1*, *HAND2*, *TGFBR3*, *ERBB3*) and protein (HAND2) levels by qRT-PCR and Western blot respectively after cSrc inhibition (**Fig. 3G**). We also confirmed loss of RBM10 tyrosine phosphorylation on cSrc inhibition in both day 5 and day 8 isoproterenol induced hypertrophic heart by immunoprecipitation of RBM10 from respective heart tissues (**Fig. 3I**).

These results were further validated in H9c2 cells after treatment with isoproterenol at various intervals in the presence and absence of cSrc inhibitor. Interestingly, we observed a significant increase in the cell size and actin filament reorganisation from 12- to 18-hrs post isoproterenol treatment. However, in the presence of cSrc inhibition, H9c2 cells become significantly hypertrophic 6- to 12-hrs post

isoproterenol treatment. Similarly, significant reduction in the SERCA2A level was visible 6-hrs post isoproterenol treatment whereas in the absence it was visible 12-hrs post isoproterenol treatment (**Fig. 3J**). We also saw early reductions of mRNA levels of molecular marker *SERCA2A* and RBM10 target *HAND2* on cSrc inhibition after isoproterenol treatment (**Fig. 3K**). Taken together, these results indicate that cSrc-inhibition accentuates hypertrophic induction in both animal heart model and cellular H9c2 hypertrophy model.

6. cSRC-inhibition advances hypertrophy induction in the isoproterenol administered rat heart

While we observed significant hypertrophy on day 8 of isoproterenol administration, heart became significantly hypertrophic after 5 days upon cSrc inhibition (**Fig. 3A-I**). Strikingly, we saw similar reductions in IVSd and LVPWd or inductions in LVFS and LVEF as on day 8 of isoproterenol administration on day 5 after cSrc inhibition. Likewise, we also saw thickened ventricular wall in the cross-section and increased heart size after cSrc inhibition of day 5 after cSrc inhibition comparable to that of day 8 isoproterenol treatment (**Fig. 3E-F**). Similarly, total protein content and changes in the molecular markers as seen on day 8 were observed on day 5 post-cSrc inhibition in both Western (increase in BNP, ANP, SKA and decrease in SERCA2A) and qRT-PCR analysis (increase in *BNP, ANP, β-MHC*, or decrease in *SERCA2A* and *α-MHC*) (**Fig. 3G-H**). However, isoproterenol treatment had only a feeble effect on both hemodynamic and molecular changes on day 5 in the absence of cSrc inhibition. Nevertheless, in both day 5 and day 8 samples, there was accentuation in these parameters of the heart function (**Fig. 3G-H**). However, reduction in the expression of RBM10 was equally visible at day 8 versus day 5 of isoproterenol administration after cSrc inhibition (**Fig. 3G**). Together these results indicate that cSrc-mediated RBM10 phosphorylation regulates hypertrophy in the heart and that cSrc inhibition results in early attainment of hypertrophy.

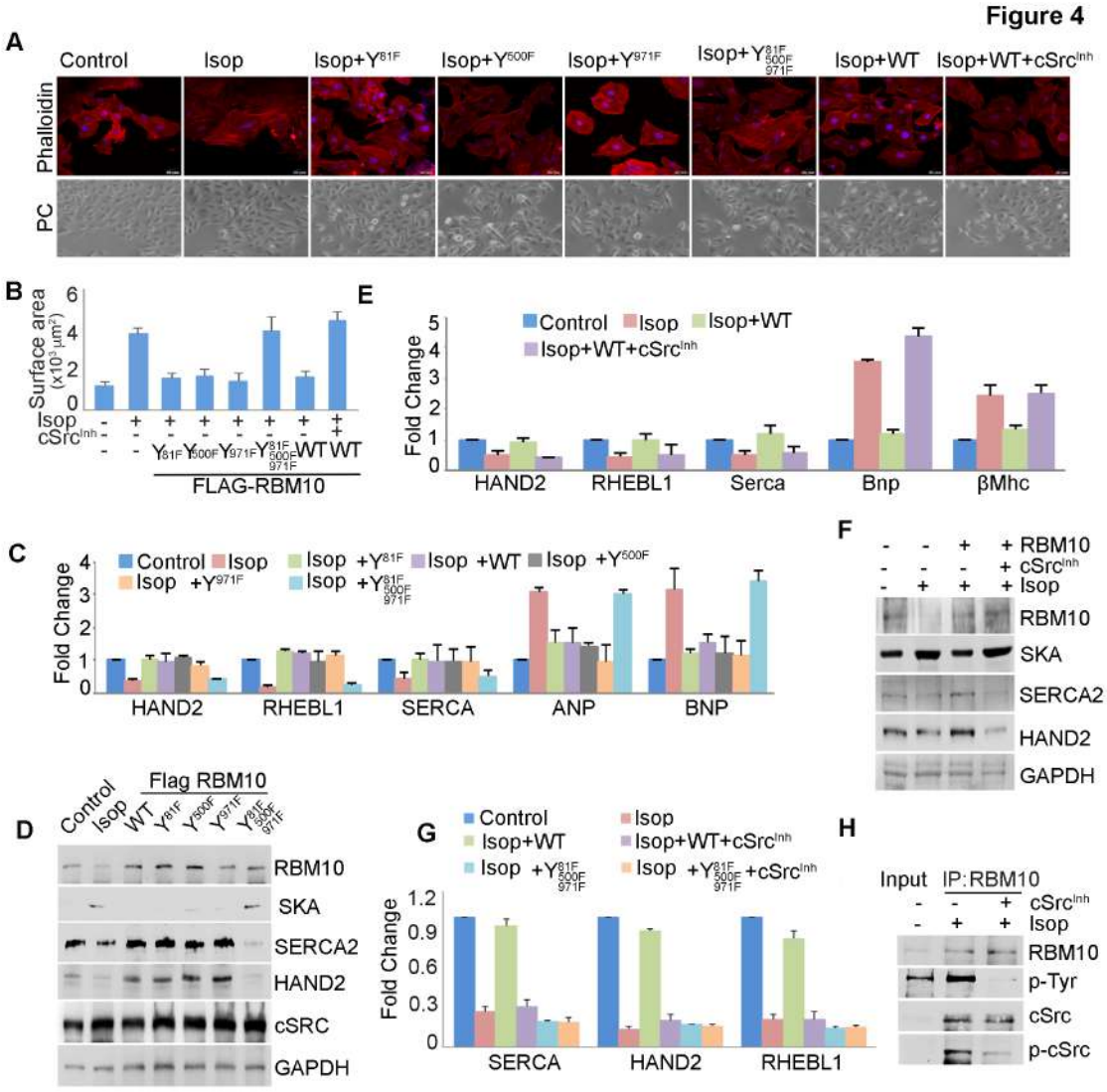

Fig. 4: RBM10 re-expression failed to restore hypertrophic induction in the presence of triple-phopsho mutation or cSrc-inhibition in H9c2 cells. (**A**) Phase contrast (PC) and IF imaging of phalloidin stained H9c2 cells after treatment with isoproterenol (100 µM for 48-hr), and rescue with wild type and various phospho-mutant RBM10 as indicated. (**B**) Quantification of cell surface area of the phalloidin stained H9c2 cells in A. Error bar represents SEM. Average cell surface area was measured for >50 cells per experiment for n>3 independent experiments (p values <0.01 in all conditions). (**C**) qRT-PCR analysis of mRNA levels of various RBM10 targets and hypertrophic markers as indicated from H9c2 cells under the same conditions as in A. Error bar represents standard error mean (SEM) of n=3 independent experiments. [p values (<0.008 in all conditions for *HAND2, SERCA2A* and *ANP*), (<0.02 in all

conditions for *BNP* and *RHEBL1*)] relative to control. (**D**) Western blot analysis of RBM10, RBM10 target HAND2, hypertrophic markers (SERCA2A and SKA), and cSrc from H9c2 cells under the same conditions as in C. Each blot is representative of n=3 independent experiments. (**E**) qRT-PCR analysis of RBM10 target mRNA and hypertrophic markers as indicated from total RNA isolated from H9c2 cells after treatment with isoproterenol and rescue with either wild type or triple phospho mutant RBM10 in the presence and absence of cSrc inhibition. Error bar represents standard error mean (SEM) of n=3 independent experiments. [p values (<0.01 in all conditions except isoproterenol + WT RBM10 expression for *HAND2*), (<0.02 in all conditions except isoproterenol + WT RBM10 expression for *BNP, SERCA2A* and *RHEBL1*), and (<0.02 for *β-MHC*] relative to control. Isoproterenol + WT RBM10 expression values did not show significant difference relative to control in all genes. (**F**) Western blot analysis of RBM10 target HAND2 and hypertrophic marker SERCA2A, SKA and RBM10 from H9c2 cells under the conditions as in F. **(G)** qRT-PCR analysis of RBM10 target mRNAs from H9c2 cells after treatment with isoproterenol and re-expression of WT and triple phopsho-mutant RBM10 in the presence and absence of cSrc inhibition. Error bar represents standard error mean (SEM) of n=3 independent experiments. [p values (<0.02 for *SERCA2A,* 0.05 for *HAND2,* and 0.007 for *RHEBL1* in all conditions relative to control). (**H**) Immunoprecipitation of RBM10 from H9c2 cells after isoproterenol treatment in the presence and absence of rescue with wild type or triple phospho-mutant RBM10 followed by Western blot analysis with RBM10 and phospho-tyrosine specific antibodies.

7. Restoration of RBM10 levels by ectopic expression or endogenously by ERK inhibition failed to reverse isoproterenol-induced hypertrophy after cSrc inhibition

We have shown that ectopic re-expression of RBM10 rescues cellular and molecular changes associated with hypertrophic induction in H9c2 cells. To further confirm the role of cSrc-mediated RBM10 phosphorylation on myocyte hypertrophy, we first re-expressed various phospho-mutants of RBM10 and wild type RBM10 in H9c2 cells after isoproterenol treatment in the presence and absence of cSrc inhibition. As reported earlier, wild type RBM10 expression reversed the increase cell size and molecular changes of hypertrophic phenotype in H9c2 cells (**Fig. 4A-D**). The increased cell size on isoproterenol treatment was restored to near normal level on the re-expression (**Fig. 4A-B**). Similarly, reduced expression of SERCA2A or increased ANP and BNP protein levels were also brought back to near control levels (**Fig. 4C-D**). However, re-expression RBM10 triple-phospho mutant failed to reverse the same molecular and

cellular changes incurred during hypertrophy in contrast to the wild type RBM10 (**Fig. 4A-D**). Expression of individual phospho mutations rescued the hypertrophic phenotype similar to the wild type RBM10 (**Fig. 4A-D**). In line with these molecular changes, RBM10 re-expression resulted in a significant reversal of target mRNA and protein expressions after isoproterenol treatment in H9c2 cells (**Fig. 4C-D**). However, in the presence of the triple-phospho mutation, there was no significant reversal of the target gene expression on RBM10 re-expression (**Fig. 4C-D**). Similarly, in the presence of cSrc inhibition, wild type RBM10 expression did not rescue cellular and molecular changes incurred on hypertrophic induction similar to RBM10 triple phospho-mutation (**Fig. 4A-B, E-F**). Loss of RBM10 targets mRNA (*HAND2*, *RHEBL1*) and protein (HAND2) expressions on hypertrophic induction were equally unaltered by RBM10 expression in the presence of cSrc inhibition (**Fig. 4E-F**). There was no further effect of cSrc inhibition on RBM10 having triple-phospho mutation (**Fig. 4G**). Further, we confirmed loss of RBM10 phosphorylation after cSrc inhibition (**Fig. 4H**).

Previously, we showed that ERK mediated phosphorylation resulted in the down regulation of RBM10 during hypertrophy[51]. Inhibition of ERK in isoproterenol-induced hypertrophic myocyte restored RBM10 expression and reverses myocyte hypertrophy in both animal and cellular model[8, 51, 65]. To confirm the implication of cSrc-mediated RBM10 phosphorylation on hypertrophic myocyte, we first restored endogenous RBM10 expression by ERK inhibition in both animal heart and H9c2 cells after isoproterenol administration. In H9c2 cell line, we saw endogenous RBM10 expression restored on ERK inhibition (**Fig. 5A-B**). Inhibition of cSrc did not affect RBM10 level in the presence of ERK inhibition. Concomitantly, we found that molecular changes on isoproterenol treatment (increased *BNP*, or decreased *SERCA2A* and *α-MHC* in mRNA and SERCA2A in protein) were reversed by ERK inhibition similar to RBM10 re-expression (**Fig. 5A-B**). Strikingly, in the presence of cSrc inhibitor treatment, ERK inhibition failed to restore molecular changes occurred in myocyte hypertrophy while RBM10 expression was restored (**Fig. 5A-B**). Similar effect of ERK inhibition was also

observed on RBM10 targets mRNA (*HAND2*, *TGFBR3*, *RHEBL1*) and protein (HAND2) expression after cSrc inhibition (**Fig. 5A, C**). Yet, the same expressions were not altered in the presence of cSrc inhibitor treatment after ERK inhibition (**Fig. 5A, C**). Concomitantly, the induced cell size on isoproterenol treatment was restored to control level on ERK inhibition but not in the presence of cSrc inhibitor treatment (**Fig. 5D-E**).

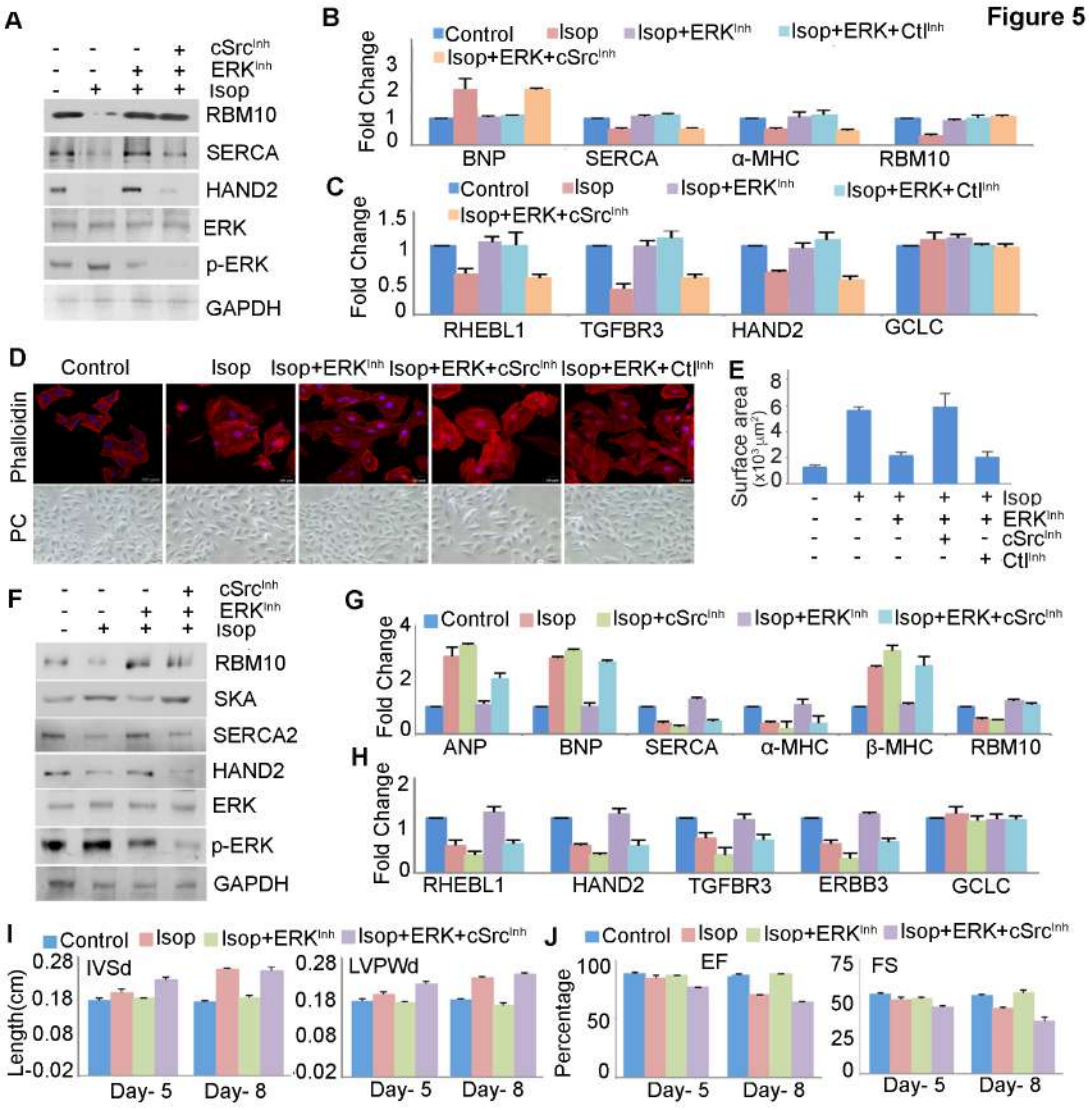

Fig. 5: Restoration of RBM10 levels by ERK inhibition failed to reverse isoproterenol-induced hypertrophy after cSrc inhibition. (**A**) Western blot analysis of

RBM10, hypertrophic markers (SERCA2A, SKA) and cSrc from H9c2 cells after treatment with isoproterenol in the presence or absence of ERK and cSrc inhibition as indicated. Each blot is representative of n=3 independents Western experiments. (**B**) qRT-PCR analysis of mRNA levels of various hypertrophic markers from H9c2 cells treated with isoproterenol after ERK inhibition in the presence and absence of control or cSrc inhibition as indicated. Error bar represents standard error mean (SEM) of n=3 independent experiments. [p values (<0.03 in all conditions except isoproterenol + ERK^{Inh} and Ctl^{Inh} for *BNP*), (<0.02 in all conditions except isoproterenol + WT RBM10 expression for *BNP, SERCA2A* and *RHEBL1*), and (<0.02 for *SERCA2A* and *α-MHC*) relative to control. Isoproterenol + ERK^{Inh} and Ctl^{Inh} values did not show significant difference relative to control in all genes]. (**C**) qRT-PCR analysis of mRNA levels of various targets of RBM10 from H9c2 cells under the same conditions as in B. Error bar represents standard error mean (SEM) of n=3 independent experiments. [p values (<0.03 for TGFBR3, <0.009 for *RHEBL1* and *HAND2* in all conditions except isoproterenol + ERK^{Inh} and Ctl^{Inh}) relative to control. Isoproterenol + ERK^{Inh} and Ctl^{Inh} values did not show significant difference relative to control in all genes. (**D**) Phase contrast (PC) and IF imaging of phalloidin stained H9c2 cells after treatment with isoproterenol (100 μM for 48 h) under the same condition as in B. Quantification of the cell surface area is shown in (**E**) Quantification of cell surface area of the phalloidin stained H9c2 cells in D. Average cell surface area was measured for >50 cells per experiment for n>3 independent experiments (P value <0.002 in all conditions). (**F**) Western blot analysis of RBM10, hypertrophic markers and target proteins from control and isoproterenol induced hypertrophic heart in the presence and absence of ERK or cSrc inhibition as indicated. (**G**) qRT-PCR analysis of mRNA levels of various hypertrophic markers from from control and isoproterenol induced hypertrophic heart after ERK inhibition in the presence and absence of control or cSrc inhibition as indicated. Error bar represents standard error mean (SEM) of n=3 independent experiments. [p values (<0.02 in all conditions except isoproterenol + ERK^{Inh} for *BNP* and *ANP*), (<0.02 in all conditions except isoproterenol + WT RBM10 expression for *BNP, SERCA2A* and *RHEBL1*), and (<0.009 for *SERCA2A* and *α-MHC*) relative to control. Isoproterenol + ERK^{Inh} values did not show significant difference relative to control in all genes. (**H**) qRT-PCR analysis of mRNA levels of various RBM10 target mRNAs from control and isoproterenol induced hypertrophic heart under the same conditions as in G as indicated. Error bar represents standard error mean (SEM) of n=3 independent experiments. [p values (<0.009 in all conditions except isoproterenol + ERK^{Inh} for *RHEBL2, TGFBR3* and *HAND2*), (<0.01 in all conditions except isoproterenol + ERK^{Inh} for *ERBB3*) relative to control. Isoproterenol + ERK^{Inh} values did not show significant difference relative to control in all genes. (**I**) Measurement of interventricular septum diastole (IVSd) and left ventricular posterior wall thickness (LVPWD) of control and hypertrophic animals under the similar conditions as in F. (**J**) Measurement of left ventricular ejection fraction (LVEF %) and left ventricular fraction shortening (LVFS %) of control and hypertrophic animals under the similar conditions as in F (n = 5 per group. Error bar represents SEM). (p values <0.001 for day 5 and 0.004 for day 8 in the case of IVSd, and <0.005 for day 5 and 0.001 for day 8 in the case of LVPWD in all conditions).

In the animal heart model, we focused on day 5 and day 8 of isoproterenol administration where we inhibited ERK in the presence and absence of cSrc inhibitor treatment. As reported earlier, we observed significant reversal of RBM10 protein level near to control in the animal heart (**Fig. 5F-G**). Concomitantly, we observed marked reversal of altered molecular markers of isoproterenol-induced hypertrophic heart after ERK inhibition (**Fig. 5F-G**). Strikingly, while ERK inhibition restored RBM10 expression, it failed to rescue molecular changes in hypertrophic heart in the presence of cSrc inhibition (**Fig. 5F-G**). Changes in the levels of protein (SERCA2A, SKA) or mRNA (*SERCA2A* or *α-MHC*, *ANP*, *BNP, β-MHC*) on hypertrophic induction were rescued by ERK inhibition but not in the presence of cSrc inhibition (**Fig. 5F-G**). In agreement with these finding, ERK inhibition did not show significant effect on the changes in the expression of RBM10 target mRNAs (*RHEBL1*, *HAND2*, *TGFBR3*, *ERBB3*) and protein (HAND2) after cSrc inhibition despite the presence of normal RBM10 levels (**Fig. 5F, H**). We saw induction of phosphorylation on isoproterenol treatment and on ERK inhibition that was lost on cSrc treatment consistent with subsequent molecular changes in the hypertrophic heart. These results further strengthen our finding that cSrc-mediated RBM10 phosphorylation regulates anti-hypertrophy function in the heart. Similar results were obtained in the assessment of ventricular and hemodynamic parameters of the heart as well. In the day 8 hypertrophic animal heart, there was ~20% increase in IVSd and LVPWd and >40% decrease in both LVFS and LVEF on isoproterenol treatment that was reversed to near normal level on ERK inhibition (**Fig. 5I-J**). However, there were no significant changes on ERK inhibitor treatment after cSrc inhibition in these parameters on the same hypertrophic heart (**Fig. 5I-J**). Similar effect of cSrc inhibition was visible on total protein level, heart size and cross sectional area of ERK inhibited hypertrophic heart (**Fig. 3E-F**). However, on the day 5 animal, isoproterenol had little effect on the molecular and hemodynamic changes

that was heightened on cSrc inhibition akin to that in day 8 hypertrophic heart (**Fig. 5F-J**). ERK inhibition also did not show marked alteration on the hypertrophy parameters of the cSrc inhibited hypertrophic heart (**Fig. 5F-J**). Our findings confirm that cSrc mediated phosphorylation of RBM10 mediates anti-hypertrophy function to regulate myocyte hypertrophy.

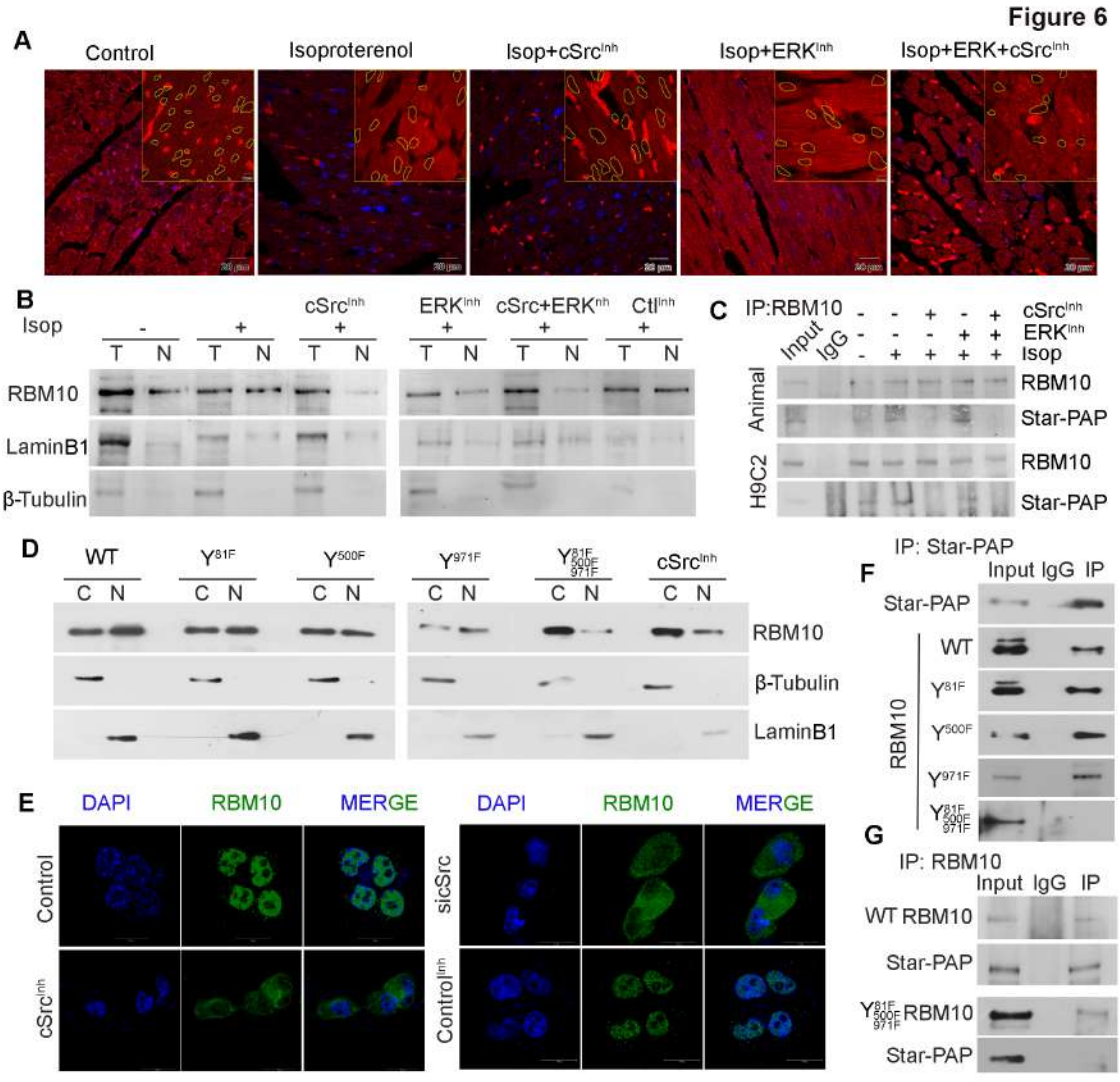

Fig. 6: RBM10 phosphorylation enables RBM10 nuclear localisation and Star-PAP interaction during hypertrophy induction in the heart. (A) Immunostaining of RBM10

(red) along with DAPI (blue) from the heart tissue sections of animals as in 5G. Inset shows zoomed area of the tissue section with the nuclear regions circled with yellow line for comparison of the nuclear RBM10 (red) content in all conditions. Quantification of both total RBM10 level and nuclear content is shown in Supplementary Fig. E-F. For clarity of the difference in the nuclear RBM10 content under different conditions, the contrast of each images were increased to the similar brightness (inset). (**B**) Nuclear fractionation and assessment of RBM10 level in the nucleus expressed over total protein from tissue samples as in A. (**C**) Immunoprecipitation of RBM10 from animal tissues and H9c2 cells as in A followed by Western blot analysis of RBM10 and Star-PAP as indicated. Input = 10% of total IP sample. (**D**) Immunoprecipitation and Western analysis as in C but from H9c2 cells after isoproterenol treatment in the presence and absence of cSrc or ERK inhibition as indicated. Input = 10% of total IP sample. (**E**) Immunofluorescence imaging of RBM10 and DAPI in the HEK293 cells under the conditions as indicated. (**F**) Immunoprecipitation of Star-PAP from HEK293 cells after transfection with wild type and various phosphomutant RBM10 as indicated followed by Western analysis of Star-PAP and FLAG-RBM10. Input = 10% of total IP sample. (**G**) Immunoprecipitation of RBM10 using antibody against FLAG-epitope tag from HEK293 cells expressing wild type and triple-phospho mutant RBM10 followed by Western blot analysis of Star-PAP and RBM10 as indicated.

8. RBM10 phosphorylation enables RBM10 nuclear localisation and Star-PAP interaction that regulates anti-hypertrophy gene program in the heart

To understand the mechanism how cSrc-mediated RBM10 tyrosine phosphorylation controls anti-hypertrophy function in the heart, we assessed RBM10 nuclear localisation and Star-PAP interaction. We first analysed RBM10 nuclear localisation in the heart tissue samples of normal and isoproterenol induced hypertrophic heart in the presence and absence of cSrc or ERK kinase inhibitors (**Fig. 6A**). We saw induced RBM10 nuclear localisation on isoproterenol administered animal heart compared to normal animal heart that was lost on cSrc inhibition (**Fig. 6A**). While ERK inhibition induced RBM10 levels, its nuclear localisation was not proportionately increased in the presence of cSrc treatment consistent with the loss of RBM10 phosphorylation on the inhibition (**Fig. 6A**). Nevertheless, in the absence of cSrc inhibitor, ERK inhibition resulted in increased nuclear localisation of RBM10 in the hypertrophic heart tissue compared to control tissues (**Fig. 6A**). To further confirm this,

we fractionated nucleus from the tissue samples of hypertrophic heart under the same conditions and assessed nuclear to total protein ratio of RBM10. Consistently, we observed increased nuclear localisation over total protein of RBM10 in hypertrophic heart tissues from the normal tissues (**Fig. 6B**). cSrc inhibition resulted in the loss of the nuclear to total protein ratio of RBM10 in the same tissues (**Fig. 6B**). In agreement with the immunofluorescence observation, while ERK inhibition could increase ratio of RBM10 nuclear content over total, it failed to stimulate the reduction of RBM10 nuclear content after cSrc inhibition (**Fig. 6B**). This finding suggests that RBM10 nuclear localisation during hypertrophy is facilitated through cSrc mediated phosphorylation of RBM10. Further, we analysed RBM10 interaction with Star-PAP from both in vivo hypertrophic heart and cellular hypertrophic H9c2 cells by immunoprecipitation of RBM10 and Star-PAP. Immunoprecipitation of RBM10 followed by Western analysis of Star-PAP revealed an increased interaction on ERK inhibition but a loss of interaction on cSrc inhibition (**Fig. 6C**). The loss of interaction on cSrc inhibition was not rescued by ERK inhibition consistent with the diminished RBM10 phosphorylation on cSrc inhibition (**Fig. 6C**). Consistently, immunoprecipitation from the H9c2 cells showed induced Star-PAP-RBM10 interaction during hypertrophy that was lost on cSrc inhibition (**Fig. 6C**). Our findings indicate that cSrc mediated phosphorylation of RBM10 regulates RBM10 nuclear localisation and Star-PAP interaction during hypertrophy induction.

To affirm the role of RBM10 phosphorylation on its nuclear localisation and Star-PAP interaction, we employed HEK293 cells and tested by immunofluorescence, immunoprecipitation and nuclear fractionations (**Fig. 6D-G**). First, in the nuclear fractionation, we detected wild type RBM10 in both nuclear and cytoplasmic fractions with a higher percentage in the nuclear fraction (**Fig. 6E**). However, triple-phospho mutation on RBM10 resulted in a dramatic reduction in the nuclear fraction of RBM10 (**Fig. 6E**). The same was also seen consistently on cSrc inhibition (**Fig. 6E**). However, individual phospho mutations were equally distributed in both nuclear and cytoplasmic fractions similar to that of wild type RBM10 (**Fig. 6E**). This observation was further

confirmed in immunofluorescence experiments, where we observed largely nuclear speckle localisation of RBM10. This localisation was lost on cSrc inhibition or siRNA mediated knockdown, and on the mutation of three tyrosine residues that are phosphorylated by cSrc (**Fig. 6E**). Together, these results signify that RBM10 nuclear localisation requires cSrc-mediated phosphorylation of tyrosine residues that in turn controls anti-hypertrophy function in the heart. Further, immunoprecipitation experiment of RBM10 showed that Star-PAP interacts with wild type RBM10 or individual phospho mutations but not with the triple-phospho mutant RMB10 (**Fig. 6F**). This was corroborated with reverse immunoprecipitation of Star-PAP followed by Western analysis of RBM10 demonstrating the requirement of triple tyrosine phosphorylation of RBM10 on Star-PAP-RBM10 interaction (**Fig. 6G**). Together, these results reveal that RBM10 phosphorylation by cSrc regulates both RBM10 nuclear localisation and Star-PAP interaction that in turn will control anti-hypertrophy gene program in the heart.

DISCUSSION

RNA binding proteins are extensively studied in different disease contexts [14, 26], here we explore the function of RBM10 in the case of cardiac hypertrophy an antecedent condition to heart failure that requires cSrc mediated phosphorylation[66]. RBM10 is a well-established splicing regulator that is involved in various cellular functions and complex diseases, particularly in cancer progression[29]. We reported a splicing independent function that works with a non-canonical poly(A) polymerase Star-PAP and acts as a central regulator of anti-hypertrophy gene program in the heart[37, 51]. However, how RBM10 mediates its function or its regulation is still unknown. Several post translational modifications including phosphorylation, acetylation, ubiquitinylation or methylation at different amino acid residues on the RBM10 primary structure are being proposed [1, 10, 23, 62]. Particularly, RBM10 is believed to be phosphorylated at multiple sites including serine, threonine, and tyrosine residues [3, 15, 54]. Yet, the

biological significance of such modifications or how such modifications affect RBM10 function, activity or RBM10-related cellular events is largely unknown. Recent study has highlighted the significance of CDK2 mediated phosphorylation of RBM10 at serine 89 to generate wild type BRCA1 spliced transcript[53]. In this study, we have demonstrated three tyrosine residues phosphorylated by proto-oncogene cSrc, and are induced during cardiac hypertrophy to regulate heart failure. This induction stems from inherent activation of cSrc tyrosine kinase during hypertrophy [66]. Phosphorylation of RBM10 controls its nuclear localisation and interaction with Star-PAP. Thus, cSrc-mediated phosphorylation arbitrates RBM10 anti-hypertrophy function and helps maintain a normal heart. Loss of RBM10 phosphorylation or inhibition of cSrc compromises anti-hypertrophy gene program in the heart that results in cardiac hypertrophy. A model how cSrc-mediated RBM10 phosphorylation regulates myocyte hypertrophy in the heart is shown in **Fig. 7**.

What is the molecular role of the three-tyrosine phosphorylation in RBM10 biology? We have found its involvement in at least two aspects of RBM10 molecular function - nuclear localisation and co-regulator Star-PAP interaction, both are critical for RBM10-mediated target mRNA processing[37, 51]. Yet, the mechanism how the three-tyrosine phosphorylation regulates these two aspects of RBM10 molecular activity are still unclear. RBM10 has three nuclear localisation signals - one at the C-terminus close to the RBM10 G-PATCH domain, other two being RRM1 and OCRE domain that shows NLS activity[29, 46, 49]. The three-phosphorylation sites exist in a very close proximity to these NLSs (one at the RRM1 domain, the other two are at the OCRE and the G-PATCH domain)[12, 49]. Interestingly, both Star-PAP interaction and nuclear localisation require abrogation of all the three-phosphorylation sites to fully compromise RBM10 nuclear localisation. It is likely that any one or two of NLSs could aid in both the functions provided they are phosphorylated[51]. This suggests a potential cooperation of the phosphorylation sites that could induce structural changes affecting the interaction or localisation. Further structural studies are required to understand how these

phosphorylations co-operate and co-ordinate the three NLSs to regulate RBM10 nuclear localisation or induces overall structural changes to regulate Star-PAP interaction.

Figure 7

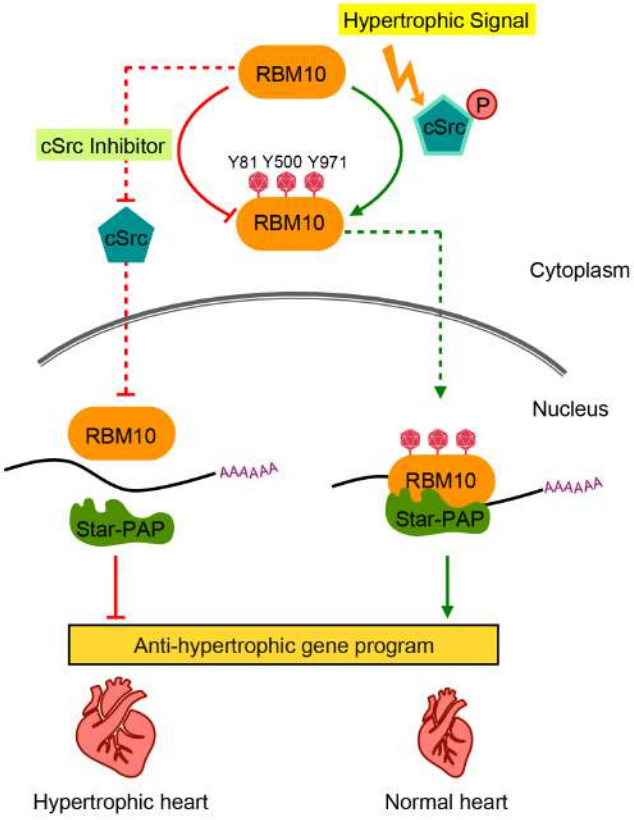

Fig. 7: Model depicting how cSrc-mediated RBM10 phosphorylation regulates RBM10 nuclear localization and Star-PAP interaction to control anti-hypertrophy gene program in cardiac hypertrophy in the animal heart.

RBM10 is required for Star-PAP cleavage and polyadenylation complex assembly on target mRNAs where RBM10 interaction with Star-PAP guides Star-PAP complex on specific target mRNAs[37, 51]. Thus, phosphorylation of RBM10 by cSrc will regulate the processing reaction through availability of nuclear RBM10 pool. Moreover, we have shown that Star-PAP interacts only with the phosphorylated RBM10 and not with non-phosphorylated RBM10. Thus, phosphorylation of RBM10 will be involved in the recruitment of Star-PAP and assembly of the Star-PAP processing complex on target mRNAs. This regulates anti-hypertrophy gene program in the heart thus controlling progression to heart failure[51]. However, Star-PAP regulates multiple cellular functions such as DNA damage, oxidative stress response, apoptosis, tumerogenesis and cellular processes in cancer progression such as proliferation, invasion or migration [40, 44, 52, 64, 75]. It is still unclear if cSrc mediated tyrosine phosphorylation of RBM10 will regulate these aspects of Star-PAP function or will it be limited to regulation of anti-hypertrophy genes in the heart. Moreover, role of RBM10 phosphorylation on other aspects of RBM10 functions than the non-canonical role in the 3′-end formation in the heart are yet to be studied. RBM10 primarily regulates alternative splicing and controls several cellular functions including inflammation, embryonic development, apoptosis, and disease such as cancer [5, 31, 34, 45, 58, 70]. Splicing and alternative splicing occurs primarily inside the nucleus[24]. Given the role of RBM10 phosphorylation in nuclear localisation, it is likely that RBM10 mediated splicing of pre-mRNAs also require RBM10 phosphorylation. However, future studies are required to fully ascertain how phosphorylation regulates this aspect of RBM10 activity, or (if any) specificity in the regulation of different RBM10 functions by cSrc-mediated phosphorylation.

Here, we have established that RBM10 tyrosine phosphorylation regulates anti-hypertrophy gene program regulating overall cardiac hypertrophy. However, RBM10 is down regulated downstream of hypertrophy signal compromising target mRNA expression[51]. The implication of RBM10 phosphorylation after heart becomes hypertrophic are still unclear. Potentially, induction of residual RBM10 phosphorylation

will enable RBM10 anti-hypertrophy function protecting against further accentuation of hypertrophy that could lead to heart failure. This is demonstrated by our results that show accentuation of myocyte hypertrophy on mutation of the three-tyrosine phosphorylation sites to phenylalanine. Thus, regulation of heart failure progression will be tightly linked with cSrc mediated RBM10 phosphorylation. Therefore, RBM10 phosphorylation or cSrc kinase - RBM10 axis could potentially be employed to target in the therapeutics for heart failure prevention. Our results indicate that RBM10-mediated hypertrophy works through two of the kinases cSrc and ERK that have well established roles in the regulation of cardiac hypertrophy and heart failure[65, 66, 73, 76]. Alternatively, it is likely that these two kinases also function in part through RBM10 to regulate hypertrophy gene program among other additional targets of these kinases [65]. At present, the exact mechanism and the implication how these kinases and RBM10 co-operate to regulate hypertrophy and heart failure remains to be elucidated.

IMPACT OF THE RESEARCH IN THE ADVANCEMENT OF KNOWLEDGE OR BENEFIT TO MANKIND

RBM10 is an RNA binding protein that regulates both splicing and RNA 3'-end maturation and controls several human diseases. RBM10 protein has gained credible amount of significance in the recent years. A 60% of the total of results of the PubMed search have come up only since 2020. This implies an increased interest towards this molecule; many studies have implied different mutation of RBM10 in different disease conditions. A recent study in Acute myeloid leukaemia has shown the significance of RBM10 in ventoclax drug resistance and that co-targeting RBM10 can act as a potential therapeutic regime for drug resistance in chemotherapy. Our finding, on the other hand, sheds light on the role of RBM10 in cardiac hypertrophy, and antecedent condition to heart failure and the mechanism by which RBM10 regulates cardiac hypertrophy. My work has identified a regulatory switch for RBM10 that is mediated by cSrc kinase to

arbitrate its anti-hypertrophy function in the heart. This phosphorylation is essential for nuclear localisation of RBM10 and its interaction with the non-canonical polymerase Star-PAP. Nuclear localisation of RBM10 hold immense importance as it facilitates the primary role of RBM10 as splicing factor and also as a regulator of 3'-end processing with Star-PAP. While re-expression of RBM10 in hypertrophied cardiomyoblast can rescue the condition, we find that phosphorylation is essential to rescue the hypertrophied state to normal heart. Thus, this has direct clinical relevance in the heart failure management. Synthesising small molecules targeting and activating the RBM10 cSrc nexus could be a promising strategy to manage cardiac hypertrophy and prevent progression to heart failure. In conclusion, the heart cells undergo tremendous functional adaptation in response to stress and other stimuli. These remodelling events are intricately orchestrated by various RNA binding protein (RBPs) that act as potent regulator molecules for pathogenesis of complex diseases. Thus, characterizing active and functional RBM10 molecule in the cardiomyocytes will be of immense value in the evolving therapeutic strategies to combat various cardiovascular diseases.

LITERATURE REFERENCES

1. Akimov V, Barrio-Hernandez I, Hansen SVF, Hallenborg P, Pedersen AK, Bekker-Jensen DB, Puglia M, Christensen SDK, Vanselow JT, Nielsen MM, Kratchmarova I, Kelstrup CD, Olsen JV, Blagoev B (2018) UbiSite approach for comprehensive mapping of lysine and N-terminal ubiquitination sites. Nat Struct Mol Biol 25:631-640 doi:10.1038/s41594-018-0084-y
2. Alper O, Bowden ET (2005) Novel insights into c-Src. Curr Pharm Des 11:1119-1130 doi:10.2174/1381612053507576
3. Amanchy R, Zhong J, Molina H, Chaerkady R, Iwahori A, Kalume DE, Gronborg M, Joore J, Cope L, Pandey A (2008) Identification of c-Src tyrosine kinase substrates using mass spectrometry and peptide microarrays. J Proteome Res 7:3900-3910 doi:10.1021/pr800198w
4. Antonello ZA, Hsu N, Bhasin M, Roti G, Joshi M, Van Hummelen P, Ye E, Lo AS, Karumanchi SA, Bryke CR, Nucera C (2017) Vemurafenib-resistance via de novo RBM genes mutations and chromosome 5 aberrations is overcome by combined therapy with palbociclib in thyroid carcinoma with BRAF(V600E). Oncotarget 8:84743-84760 doi:10.18632/oncotarget.21262

5. Bechara EG, Sebestyen E, Bernardis I, Eyras E, Valcarcel J (2013) RBM5, 6, and 10 differentially regulate NUMB alternative splicing to control cancer cell proliferation. Mol Cell 52:720-733 doi:10.1016/j.molcel.2013.11.010
6. Blom N, Gammeltoft S, Brunak S (1999) Sequence and structure-based prediction of eukaryotic protein phosphorylation sites. J Mol Biol 294:1351-1362 doi:10.1006/jmbi.1999.3310
7. Cao Y, Di X, Zhang Q, Li R, Wang K (2021) RBM10 Regulates Tumor Apoptosis, Proliferation, and Metastasis. Front Oncol 11:603932 doi:10.3389/fonc.2021.603932
8. Cao YY, Li K, Li Y, Tian XT, Ba HX, Wang A, Li XH (2020) Dendrobium candidum aqueous extract attenuates isoproterenol-induced cardiac hypertrophy through the ERK signalling pathway. Pharm Biol 58:176-183 doi:10.1080/13880209.2020.1723648
9. Chadwick BP, Willard HF (2004) Multiple spatially distinct types of facultative heterochromatin on the human inactive X chromosome. Proc Natl Acad Sci U S A 101:17450-17455 doi:10.1073/pnas.0408021101
10. Choudhary C, Kumar C, Gnad F, Nielsen ML, Rehman M, Walther TC, Olsen JV, Mann M (2009) Lysine acetylation targets protein complexes and co-regulates major cellular functions. Science 325:834-840 doi:10.1126/science.1175371
11. Coleman MP, Ambrose HJ, Carrel L, Nemeth AH, Willard HF, Davies KE (1996) A novel gene, DXS8237E, lies within 20 kb upstream of UBE1 in Xp11.23 and has a different X inactivation status. Genomics 31:135-138 doi:10.1006/geno.1996.0022
12. Collins KM, Kainov YA, Christodolou E, Ray D, Morris Q, Hughes T, Taylor IA, Makeyev EV, Ramos A (2017) An RRM-ZnF RNA recognition module targets RBM10 to exonic sequences to promote exon exclusion. Nucleic Acids Res 45:6761-6774 doi:10.1093/nar/gkx225
13. Cong S, Di X, Li R, Cao Y, Jin X, Tian C, Zhao M, Wang K (2022) RBM10 regulates alternative splicing of lncRNA Neat1 to inhibit the invasion and metastasis of NSCLC. Cancer Cell Int 22:338 doi:10.1186/s12935-022-02758-w
14. Corley M, Burns MC, Yeo GW (2020) How RNA-Binding Proteins Interact with RNA: Molecules and Mechanisms. Mol Cell 78:9-29 doi:10.1016/j.molcel.2020.03.011
15. Dephoure N, Zhou C, Villen J, Beausoleil SA, Bakalarski CE, Elledge SJ, Gygi SP (2008) A quantitative atlas of mitotic phosphorylation. Proc Natl Acad Sci U S A 105:10762-10767 doi:10.1073/pnas.0805139105
16. Dorn GW, 2nd, Robbins J, Sugden PH (2003) Phenotyping hypertrophy: eschew obfuscation. Circ Res 92:1171-1175 doi:10.1161/01.RES.0000077012.11088.BC
17. Franchini KG, Torsoni AS, Soares PH, Saad MJ (2000) Early activation of the multicomponent signaling complex associated with focal adhesion kinase induced by pressure overload in the rat heart. Circ Res 87:558-565 doi:10.1161/01.res.87.7.558

18. Francis N, Behera MR, Natarajan K, Laishram RS (2023) Tyrosine phosphorylation controlled poly(A) polymerase I activity regulates general stress response in bacteria. Life Sci Alliance 6 doi:10.26508/lsa.202101148
19. Gerstberger S, Hafner M, Tuschl T (2014) A census of human RNA-binding proteins. Nat Rev Genet 15:829-845 doi:10.1038/nrg3813
20. Gorlin RJ, Cervenka J, Anderson RC, Sauk JJ, Bevis WD (1970) Robin's syndrome. A probably X-linked recessive subvariety exhibiting persistence of left superior vena cava and atrial septal defect. Am J Dis Child 119:176-178
21. Goto Y, Kimura H (2009) Inactive X chromosome-specific histone H3 modifications and CpG hypomethylation flank a chromatin boundary between an X-inactivated and an escape gene. Nucleic Acids Res 37:7416-7428 doi:10.1093/nar/gkp860
22. Guan G, Li R, Tang W, Liu T, Su Z, Wang Y, Tan J, Jiang S, Wang K (2017) Expression of RNA-binding motif 10 is associated with advanced tumor stage and malignant behaviors of lung adenocarcinoma cancer cells. Tumour Biol 39:1010428317691740 doi:10.1177/1010428317691740
23. Guo A, Gu H, Zhou J, Mulhern D, Wang Y, Lee KA, Yang V, Aguiar M, Kornhauser J, Jia X, Ren J, Beausoleil SA, Silva JC, Vemulapalli V, Bedford MT, Comb MJ (2014) Immunoaffinity enrichment and mass spectrometry analysis of protein methylation. Mol Cell Proteomics 13:372-387 doi:10.1074/mcp.O113.027870
24. Han J, Xiong J, Wang D, Fu XD (2011) Pre-mRNA splicing: where and when in the nucleus. Trends Cell Biol 21:336-343 doi:10.1016/j.tcb.2011.03.003
25. Hegele A, Kamburov A, Grossmann A, Sourlis C, Wowro S, Weimann M, Will CL, Pena V, Luhrmann R, Stelzl U (2012) Dynamic protein-protein interaction wiring of the human spliceosome. Mol Cell 45:567-580 doi:10.1016/j.molcel.2011.12.034
26. Hentze MW, Castello A, Schwarzl T, Preiss T (2018) A brave new world of RNA-binding proteins. Nat Rev Mol Cell Biol 19:327-341 doi:10.1038/nrm.2017.130
27. Hernandez J, Bechara E, Schlesinger D, Delgado J, Serrano L, Valcarcel J (2016) Tumor suppressor properties of the splicing regulatory factor RBM10. RNA Biol 13:466-472 doi:10.1080/15476286.2016.1144004
28. Ibrahimpasic T, Xu B, Landa I, Dogan S, Middha S, Seshan V, Deraje S, Carlson DL, Migliacci J, Knauf JA, Untch B, Berger MF, Morris L, Tuttle RM, Chan T, Fagin JA, Ghossein R, Ganly I (2017) Genomic Alterations in Fatal Forms of Non-Anaplastic Thyroid Cancer: Identification of MED12 and RBM10 as Novel Thyroid Cancer Genes Associated with Tumor Virulence. Clin Cancer Res 23:5970-5980 doi:10.1158/1078-0432.CCR-17-1183
29. Inoue A (2021) RBM10: Structure, functions, and associated diseases. Gene 783:145463 doi:10.1016/j.gene.2021.145463
30. Inoue A, Takahashi KP, Kimura M, Watanabe T, Morisawa S (1996) Molecular cloning of a RNA binding protein, S1-1. Nucleic Acids Res 24:2990-2997

31. Inoue A, Yamamoto N, Kimura M, Nishio K, Yamane H, Nakajima K (2014) RBM10 regulates alternative splicing. FEBS Lett 588:942-947 doi:10.1016/j.febslet.2014.01.052
32. Jin X, Di X, Wang R, Ma H, Tian C, Zhao M, Cong S, Liu J, Li R, Wang K (2019) RBM10 inhibits cell proliferation of lung adenocarcinoma via RAP1/AKT/CREB signalling pathway. J Cell Mol Med 23:3897-3904 doi:10.1111/jcmm.14263
33. Johnston JJ, Teer JK, Cherukuri PF, Hansen NF, Loftus SK, Center NIHIS, Chong K, Mullikin JC, Biesecker LG (2010) Massively parallel sequencing of exons on the X chromosome identifies RBM10 as the gene that causes a syndromic form of cleft palate. Am J Hum Genet 86:743-748 doi:10.1016/j.ajhg.2010.04.007
34. Jung JH, Lee H, Cao B, Liao P, Zeng SX, Lu H (2020) RNA-binding motif protein 10 induces apoptosis and suppresses proliferation by activating p53. Oncogene 39:1031-1040 doi:10.1038/s41388-019-1034-9
35. Just PA, Letourneur F, Pouliquen C, Dome F, Audebourg A, Biquet P, Vidaud M, Terris B, Sibony M, Pasmant E (2016) Identification by FFPE RNA-Seq of a new recurrent inversion leading to RBM10-TFE3 fusion in renal cell carcinoma with subtle TFE3 break-apart FISH pattern. Genes Chromosomes Cancer 55:541-548 doi:10.1002/gcc.22356
36. Kandala DT, Mohan N, A V, Ap S, G R, Laishram RS (2016) CstF-64 and 3'-UTR cis-element determine Star-PAP specificity for target mRNA selection by excluding PAPalpha. Nucleic Acids Res 44:811-823 doi:10.1093/nar/gkv1074
37. Koshre GR, Shaji F, Mohanan NK, Mohan N, Ali J, Laishram RS (2021) Star-PAP RNA Binding Landscape Reveals Novel Role of Star-PAP in mRNA Metabolism That Requires RBM10-RNA Association. Int J Mol Sci 22 doi:10.3390/ijms22189980
38. Kunimoto H, Inoue A, Kojima H, Yang J, Zhao H, Tsuruta D, Nakajima K (2020) RBM10 regulates centriole duplication in HepG2 cells by ectopically assembling PLK4-STIL complexes in the nucleus. Genes Cells 25:100-110 doi:10.1111/gtc.12741
39. Laishram RS, Anderson RA (2010) The poly A polymerase Star-PAP controls 3'-end cleavage by promoting CPSF interaction and specificity toward the pre-mRNA. EMBO J 29:4132-4145 doi:emboj2010287 [pii]
10.1038/emboj.2010.287
40. Laishram RS, Barlow CA, Anderson RA (2011) CKI isoforms alpha and epsilon regulate Star-PAP target messages by controlling Star-PAP poly(A) polymerase activity and phosphoinositide stimulation. Nucleic Acids Res 39:7961-7973 doi:gkr549 [pii]
10.1093/nar/gkr549
41. Laishram RS, Gowrishankar J (2007) Environmental regulation operating at the promoter clearance step of bacterial transcription. Genes Dev 21:1258-1272 doi:21/10/1258 [pii]
10.1101/gad.1520507

42. Langenickel TH, Buttgereit J, Pagel-Langenickel I, Lindner M, Monti J, Beuerlein K, Al-Saadi N, Plehm R, Popova E, Tank J, Dietz R, Willenbrock R, Bader M (2006) Cardiac hypertrophy in transgenic rats expressing a dominant-negative mutant of the natriuretic peptide receptor B. Proc Natl Acad Sci U S A 103:4735-4740 doi:10.1073/pnas.0510019103
43. Lennmyr F, Ericsson A, Gerwins P, Akterin S, Ahlstrom H, Terent A (2004) Src family kinase-inhibitor PP2 reduces focal ischemic brain injury. Acta Neurol Scand 110:175-179 doi:10.1111/j.1600-0404.2004.00306.x
44. Li W, Laishram RS, Ji Z, Barlow CA, Tian B, Anderson RA (2012) Star-PAP control of BIK expression and apoptosis is regulated by nuclear PIPKIalpha and PKCdelta signaling. Mol Cell 45:25-37 doi:S1097-2765(11)00907-5 [pii]
10.1016/j.molcel.2011.11.017
45. Loiselle JJ, Roy JG, Sutherland LC (2017) RBM10 promotes transformation-associated processes in small cell lung cancer and is directly regulated by RBM5. PLoS One 12:e0180258 doi:10.1371/journal.pone.0180258
46. Loiselle JJ, Sutherland LC (2018) RBM10: Harmful or helpful-many factors to consider. J Cell Biochem 119:3809-3818 doi:10.1002/jcb.26644
47. Magaki S, Hojat SA, Wei B, So A, Yong WH (2019) An Introduction to the Performance of Immunohistochemistry. Methods Mol Biol 1897:289-298 doi:10.1007/978-1-4939-8935-5_25
48. Majd NK, Metrus NR, Santos-Pinheiro F, Trevino CR, Fuller GN, Huse JT, Chung C, Ketonen L, Anderson MD, Penas-Prado M (2019) RBM10 truncation in astroblastoma in a patient with history of mandibular ameloblastoma: A case report. Cancer Genet 231-232:41-45 doi:10.1016/j.cancergen.2019.01.001
49. Martin BT, Serrano P, Geralt M, Wuthrich K (2016) Nuclear Magnetic Resonance Structure of a Novel Globular Domain in RBM10 Containing OCRE, the Octamer Repeat Sequence Motif. Structure 24:158-164 doi:10.1016/j.str.2015.10.029
50. Mellman DL, Gonzales ML, Song C, Barlow CA, Wang P, Kendziorski C, Anderson RA (2008) A PtdIns4,5P2-regulated nuclear poly(A) polymerase controls expression of select mRNAs. Nature 451:1013-1017 doi:nature06666 [pii]
10.1038/nature06666
51. Mohan N, Kumar V, Kandala DT, Kartha CC, Laishram RS (2018) A Splicing-Independent Function of RBM10 Controls Specific 3' UTR Processing to Regulate Cardiac Hypertrophy. Cell Rep 24:3539-3553 doi:10.1016/j.celrep.2018.08.077
52. Mohan N, Sudheesh AP, Francis N, Anderson R, Laishram RS (2015) Phosphorylation regulates the Star-PAP-PIPKIalpha interaction and directs specificity toward mRNA targets. Nucleic Acids Res 43:7005-7020 doi:10.1093/nar/gkv676
53. Nie C, Zhou XA, Zhou J, Liu Z, Gu Y, Liu W, Zhan J, Li S, Xiong Y, Zhou M, Shen Q, Wang W, Yang E, Wang J (2023) A transcription-independent mechanism

determines rapid periodic fluctuations of BRCA1 expression. EMBO J 42:e111951 doi:10.15252/embj.2022111951

54. Olsen JV, Blagoev B, Gnad F, Macek B, Kumar C, Mortensen P, Mann M (2006) Global, in vivo, and site-specific phosphorylation dynamics in signaling networks. Cell 127:635-648 doi:10.1016/j.cell.2006.09.026
55. Pfaffl MW (2001) A new mathematical model for relative quantification in real-time RT-PCR. Nucleic Acids Res 29:e45 doi:10.1093/nar/29.9.e45
56. Pozzi B, Bragado L, Mammi P, Torti MF, Gaioli N, Gebhard LG, Garcia Sola ME, Vaz-Drago R, Iglesias NG, Garcia CC, Gamarnik AV, Srebrow A (2020) Dengue virus targets RBM10 deregulating host cell splicing and innate immune response. Nucleic Acids Res 48:6824-6838 doi:10.1093/nar/gkaa340
57. Rachmin I, Tshori S, Smith Y, Oppenheim A, Marchetto S, Kay G, Foo RS, Dagan N, Golomb E, Gilon D, Borg JP, Razin E (2014) Erbin is a negative modulator of cardiac hypertrophy. Proc Natl Acad Sci U S A 111:5902-5907 doi:10.1073/pnas.1320350111
58. Rodor J, FitzPatrick DR, Eyras E, Caceres JF (2017) The RNA-binding landscape of RBM10 and its role in alternative splicing regulation in models of mouse early development. RNA Biol 14:45-57 doi:10.1080/15476286.2016.1247148
59. Serrano P, Hammond JA, Geralt M, Wuthrich K (2018) Splicing Site Recognition by Synergy of Three Domains in Splicing Factor RBM10. Biochemistry 57:1563-1567 doi:10.1021/acs.biochem.7b01242
60. Shupnik MA (2004) Crosstalk between steroid receptors and the c-Src-receptor tyrosine kinase pathways: implications for cell proliferation. Oncogene 23:7979-7989 doi:10.1038/sj.onc.1208076
61. Slama M, Susic D, Varagic J, Ahn J, Frohlich ED (2003) Echocardiographic measurement of cardiac output in rats. Am J Physiol Heart Circ Physiol 284:H691-697 doi:10.1152/ajpheart.00653.2002
62. Stes E, Laga M, Walton A, Samyn N, Timmerman E, De Smet I, Goormachtig S, Gevaert K (2014) A COFRADIC protocol to study protein ubiquitination. J Proteome Res 13:3107-3113 doi:10.1021/pr4012443
63. Sudheesh A, Mohan N, Francis N, Laishram RS, Anderson RA (2019) Star-PAP controlled alternative polyadenylation coupled poly (A) tail length regulates protein expression in hypertrophic heart. Nucleic acids research 47:10771-10787
64. Sudheesh AP, Laishram RS (2017) Nuclear phosphatidyl-inositol-phosphate type I kinase alpha coupled Star-PAP polyadenylation regulates cell invasion. Mol Cell Biol doi:10.1128/MCB.00457-17
65. Sun S, Kee HJ, Jin L, Ryu Y, Choi SY, Kim GR, Jeong MH (2018) Gentisic acid attenuates pressure overload-induced cardiac hypertrophy and fibrosis in mice through inhibition of the ERK1/2 pathway. J Cell Mol Med 22:5964-5977 doi:10.1111/jcmm.13869
66. Takeishi Y, Huang Q, Abe J, Glassman M, Che W, Lee JD, Kawakatsu H, Lawrence EG, Hoit BD, Berk BC, Walsh RA (2001) Src and multiple MAP kinase activation in cardiac hypertrophy and congestive heart failure under chronic

pressure-overload: comparison with acute mechanical stretch. J Mol Cell Cardiol 33:1637-1648 doi:10.1006/jmcc.2001.1427

67. Tse MM, Aboutabl ME, Althurwi HN, Elshenawy OH, Abdelhamid G, El-Kadi AO (2013) Cytochrome P450 epoxygenase metabolite, 14,15-EET, protects against isoproterenol-induced cellular hypertrophy in H9c2 rat cell line. Vascul Pharmacol 58:363-373 doi:10.1016/j.vph.2013.02.004
68. Wang E, Pineda JMB, Kim WJ, Chen S, Bourcier J, Stahl M, Hogg SJ, Bewersdorf JP, Han C, Singer ME, Cui D, Erickson CE, Tittley SM, Penson AV, Knorr K, Stanley RF, Rahman J, Krishnamoorthy G, Fagin JA, Creger E, McMillan E, Mak CC, Jarvis M, Bossard C, Beaupre DM, Bradley RK, Abdel-Wahab O (2023) Modulation of RNA splicing enhances response to BCL2 inhibition in leukemia. Cancer Cell 41:164-180 e168 doi:10.1016/j.ccell.2022.12.002
69. Wang LY, Xiao SJ, Kunimoto H, Tokunaga K, Kojima H, Kimura M, Yamamoto T, Yamamoto N, Zhao H, Nishio K, Tani T, Nakajima K, Sunami K, Inoue A (2021) Sequestration of RBM10 in Nuclear Bodies: Targeting Sequences and Biological Significance. Int J Mol Sci 22 doi:10.3390/ijms221910526
70. Wang Y, Gogol-Doring A, Hu H, Frohler S, Ma Y, Jens M, Maaskola J, Murakawa Y, Quedenau C, Landthaler M, Kalscheuer V, Wieczorek D, Wang Y, Hu Y, Chen W (2013) Integrative analysis revealed the molecular mechanism underlying RBM10-mediated splicing regulation. EMBO Mol Med 5:1431-1442 doi:10.1002/emmm.201302663
71. Xia QY, Wang XT, Zhan XM, Tan X, Chen H, Liu Y, Shi SS, Wang X, Wei X, Ye SB, Li R, Ma HH, Lu ZF, Zhou XJ, Rao Q (2017) Xp11 Translocation Renal Cell Carcinomas (RCCs) With RBM10-TFE3 Gene Fusion Demonstrating Melanotic Features and Overlapping Morphology With t(6;11) RCC: Interest and Diagnostic Pitfall in Detecting a Paracentric Inversion of TFE3. Am J Surg Pathol 41:663-676 doi:10.1097/PAS.0000000000000837
72. Xiao SJ, Wang LY, Kimura M, Kojima H, Kunimoto H, Nishiumi F, Yamamoto N, Nishio K, Fujimoto S, Kato T, Kitagawa S, Yamane H, Nakajima K, Inoue A (2013) S1-1/RBM10: multiplicity and cooperativity of nuclear localisation domains. Biol Cell 105:162-174 doi:10.1111/boc.201200068
73. Yamada H, Tsutsumi K, Nakazawa Y, Shibagaki Y, Hattori S, Ohta Y (2016) Src Family Tyrosine Kinase Signaling Regulates FilGAP through Association with RBM10. PLoS One 11:e0146593 doi:10.1371/journal.pone.0146593
74. Yin LL, Wen XM, Li M, Xu YM, Zhao XF, Li J, Wang XW (2018) A gene mutation in RNA-binding protein 10 is associated with lung adenocarcinoma progression and poor prognosis. Oncol Lett 16:6283-6292 doi:10.3892/ol.2018.9496
75. Yu C, Gong Y, Zhou H, Wang M, Kong L, Liu J, An T, Zhu H, Li Y (2017) Star-PAP, a poly(A) polymerase, functions as a tumor suppressor in an orthotopic human breast cancer model. Cell Death Dis 8:e2582 doi:10.1038/cddis.2016.199

76. Zhang W, Elimban V, Nijjar MS, Gupta SK, Dhalla NS (2003) Role of mitogen-activated protein kinase in cardiac hypertrophy and heart failure. Exp Clin Cardiol 8:173-183
77. Zhao J, Sun Y, Huang Y, Song F, Huang Z, Bao Y, Zuo J, Saffen D, Shao Z, Liu W, Wang Y (2017) Functional analysis reveals that RBM10 mutations contribute to lung adenocarcinoma pathogenesis by deregulating splicing. Sci Rep 7:40488 doi:10.1038/srep40488
78. Zhao Z, Li J, Shen F (2020) Protective effect of the RNA-binding protein RBM10 in hepatocellular carcinoma. Eur Rev Med Pharmacol Sci 24:6005-6013 doi:10.26355/eurrev_202006_21494

Feba Shaji

PhD Student

RGCB Trivandrum